

Spin-dependent phenomena induced by electromagnetic-hadronic interference at high energies

N. H. Buttimore

Trinity College, Dublin, Ireland

E. Gotsman

Tel-Aviv University, Ramat Aviv, Israel

E. Leader

Westfield College, London NW3, England

(Received 3 August 1977)

Beautiful interference phenomena should be seen in many spin-dependent observables for the collision of spin-half hadrons. The phenomena occur both in the collision of charged particles and in the collision of neutral particles with charged particles. Of most direct interest are the reactions $pp \rightarrow pp$, $np \rightarrow np$, and $\Lambda p \rightarrow \Lambda p$. Much information about the phases of the helicity-flip amplitudes near the forward direction can be obtained from the measurement of the interference. Detailed expressions are given for many experimental observables in the interference region, and the extraction of the hadronic amplitudes is discussed in depth. The existence of a new type of "enhanced" order- α correction to the hadronic amplitudes is exhibited and its consequences are explored. In particular the role of electromagnetically induced helicity flip outside the interference regions is stressed and shown to complicate the interpretation of the small measured values of the polarization at Fermilab energies.

I. INTRODUCTION

The interference at very small angles between electromagnetic and hadronic contributions to the scattering amplitude has long been a valuable tool in the study of the phase of the hadronic amplitude. The latter is, of course, of great interest on account of its connection via dispersion relations with the asymptotic behavior of the total cross section. An accurate determination of the real part of the forward scattering amplitude is of value both in testing the assumed analyticity of scattering amplitudes and in constraining the possible behavior of σ_{tot} at high energies.

The usual measurements only probe the interference between the hadronic forces and the classical, longest-range part of the electromagnetic interaction, namely, the Coulomb force. On quite general grounds, as indicated for example by the expression for the Lorentz force acting on a charged particle,

$$\vec{F} = e(\vec{E} + \vec{v} \times \vec{B}),$$

one would expect the relative importance of magnetic effects to grow with energy. These effects will be associated with the magnetic moments of the particles and will thus contribute to spin-flip amplitudes rather than to the nonflip amplitudes affected by the Coulomb force.

Thus at high energies we expect to see a whole range of new interference phenomena appearing most prominently in those experimental qualities that are sensitive to spin flip. Moreover, they

will be seen not only in the elastic scattering of *charged* particles, e.g., in $pp \rightarrow pp$, but also in reactions such as $np \rightarrow np$ and $\Lambda p \rightarrow \Lambda p$. The new interference measurements will provide us for the first time with a direct and absolute determination of the phases of certain spin-flip amplitudes.

It is the long-range character of the Coulomb interaction, namely, that the Coulomb potential drops off with distance like e/r , that is responsible for the extremely singular e^2/t behavior of the scattering amplitude as $t \rightarrow 0$. For a charge interacting with the magnetic field of a magnetic dipole μ , the magnetic potential drops off as μ/r^2 and the singularity in the amplitude will be less severe and of the form $e\mu/(-t)^{3/2}$. It will nonetheless give rise to quite dramatic experimental effects at very small t values. (The effective potential for the interaction of two magnetic dipoles drops off as $\mu_1\mu_2/r^3$. The corresponding amplitude is nonsingular at $t=0$, and no dramatic interference effects arise.)

The detection and measurement of such interference effects is a great experimental challenge. With the development of polarized gas-jet targets it may be possible to extend measurements down to the range $|t| \sim 10^{-5}$ (GeV/c)² and to monitor the polarization of the recoil particle, in which case the magnetic interference effects will be easily visible.

The possibility of electromagnetically induced spin flip is also of particular importance at present in view of the very small pp polarizations reported from Fermilab. Indeed, it is possible at high energies to produce polarizations of the size mea-

sured at moderately large t values, *well outside the interference region*, even if the hadronic spin flip is *zero* and the electromagnetic interaction alone is responsible for the spin flip in the reaction.

A point of special interest is the peculiarly asymmetric behavior of the spin-dependent observables in reactions such as $np \rightarrow np$. We are so used to thinking of both neutrons and protons as "nucleons" with almost identical dynamical properties that it may come as a surprise to learn that the polarization P_n of the neutron and the polarization P_p of the proton in the reaction $np \rightarrow np$ are totally different in magnitude at small t —indeed differ by a factor of 20. There is nothing mysterious in this asymmetry. The spin flip is induced by the motion of the magnetic moment of one particle in the Coulomb field of the other. If only one of the particles is charged this is an obviously asymmetric situation, and the most dramatic effects will always appear in observables that are sensitive to the spin flip of the neutral particle.

Although the origin of the asymmetry is perfectly simple, it is nevertheless a great nuisance technically since one must obviously give up the simplifications of isospin invariance when dealing with such effects. As one consequence we are forced to use six independent-helicity amplitudes in $np \rightarrow np$ rather than the customary five.

A second point of special interest in generalizing previous results to the case of spin- $\frac{1}{2}$ -spin- $\frac{1}{2}$ scattering is the question of the so called Coulomb phase. Corrections to the bare Coulomb amplitude α/t coming from higher-order electromagnetic corrections modify it to the form, roughly, $(\alpha/t)e^{i\alpha \ln(|t|b)}$, where b is a typical hadronic slope. It must be remembered that in the region of interference, the values of t , measured in $(\text{GeV}/c)^2$, are such as to make $\alpha/|t| \gtrsim 1$. Thus the higher-order terms actually provide a correction of order $\alpha \ln(|t|b)$, which for ultras small t , say $|t| \approx 10^{-5}$, is as large as 10α . A contribution of this size is considered to be an *enhanced* $O(\alpha)$ term and is usually included in the treatment of electromagnetic-hadronic interference. Indeed it is claimed¹ that measurements on the reaction $\pi^+p \rightarrow \pi^+p$ require the inclusion of the Coulomb phase in order to get agreement between the measured hadronic real part and dispersion relations; and this despite the fact that for the range of t actually used in the experiments, $\alpha \ln(|t|b)$ is never larger than about 3α .

Intuitively, because of the classical nature of the Coulomb force, one would expect the Coulomb phase to be insensitive to the spin of the particles involved. We show that this is indeed so by proving in detail that each helicity amplitude picks up the

same form of Coulomb phase. At the same time we find new, enhanced $O(\alpha)$ corrections which arise specifically through the spin structure, and which will become important in the problem of disentangling hadronic amplitudes from the experimentally measured ones at high energies. Indeed we shall show that certain amplitudes that we measure experimentally and refer to as "hadronic" amplitudes are seriously contaminated by electromagnetic corrections, and that these are important at all values of momentum transfer. A prescription is given for estimating the "pure" hadronic amplitudes from the measurements of the "contaminated" hadronic amplitudes.

Historically, the first consideration of magnetic interference effects is due to Schwinger,² who, as early as 1948, discovered that these effects could produce an almost 100% polarized beam of neutrons in np elastic scattering at very small momentum transfers. The importance of magnetic effects in a more modern context has been repeatedly stressed by Lapidus and co-workers.³ The general question of electromagnetic-hadronic interference, in particular the calculation of the Coulomb phase, has been investigated by several authors, notably, Bethe,⁴ Solov'ev,⁵ Locher,⁶ and most comprehensively by West and Yennie.⁷

The present work overlaps all these studies to some extent, but our treatment is more general and our results more detailed. Insofar as the Coulomb phase is concerned, our calculation supports the results obtained by West and Yennie.⁷ In general, our main emphasis is on the spin-dependent phenomena and our results are expressed in the modern language of helicity amplitudes. The principal aim of this paper is a comprehensive study of elastic spin- $\frac{1}{2}$ -spin- $\frac{1}{2}$ scattering at high energies in the electromagnetic-hadronic interference region.

Because of the complexity of the calculations we have tried to keep the main body of the paper free from technical detail. Thus all mathematical manipulations are relegated to the appendices.

We summarize our main results:

(a) We give expressions valid for small t for all experimental quantities of interest, including polarizations, spin-correlations parameter, etc., in the form

$$X = \frac{\alpha^2 X^{(2)}}{t^2} + \frac{\alpha}{t} [X^{(1)} - \bar{X}^{(1)} \ln|t|] + X^{(0)}$$

(where X denotes the relevant experimental quantity), and relations expressing the coefficients $X^{(0),(1),(2)}$, $\bar{X}^{(1)}$ in terms of the hadronic amplitudes and electromagnetic corrections to them. These results will enable us to determine the absolute phases of certain spin-flip amplitudes. There are

cases where it is of particular interest to have this information so as to be able to test theoretical models of high-energy scattering.

(b) We discuss the Coulomb phase in the presence of spin and show the existence of new enhanced $O(\alpha)$ corrections that could significantly affect the determination of “pure” hadronic amplitudes at high energies.

(c) We present detailed numerical results for the polarizations and spin-correlation parameters which result from magnetic effects even when *all hadronic helicity-flip amplitudes are put equal to zero*. Although the resulting magnitudes are small outside of the interference region they are, for example, in the case of the polarization, comparable to values measured at Fermilab recently. These magnetic contributions can clearly have a profound effect upon our interpretation of very high-energy measurements.

(d) We calculate the electromagnetic corrections to the hadronic amplitudes using a technique that can easily be adapted to the solution of a totally different problem, namely, the correct treatment of absorptive corrections in nucleon-nucleon scattering.

Table I shows which hadronic amplitudes are involved in the interference terms of the most interesting experimental observables.

A work about the notation used for the experimental observables is needed. Since the advent of polarized-beam-polarized-target experiments the emphasis has switched from observables which depend upon the final spins to those which depend upon the initial spins. Physicists have been extremely careless about the symbols used to denote the currently popular observables. Therefore to avoid confusion we have referred all our observables to the fundamental experimental quantity $I(\hat{a}, \hat{b}; \hat{c}, \hat{d})$, in which the unit vectors are given in the order (beam, target; scattered, recoil), and in which the possible directions of these vectors are shown in Fig. 9. (A more detailed description is given in Sec. III D.)

In Sec. II we discuss the theoretical structure of electromagnetic-hadronic interference at a general and qualitative level. The detailed results and expressions for the experimental observables in $p\bar{p} \rightarrow p\bar{p}$, $n\bar{p} \rightarrow n\bar{p}$, and $AB \rightarrow AB$, where A and B are any spin- $\frac{1}{2}$ fermions, A neutral, B charged, are presented in Sec. III. It is shown how measurements of these observables yield information on the “contaminated” hadronic amplitudes. Section IV discusses the extraction of a “pure” hadronic amplitude from the “contaminated” hadronic amplitudes.

In Appendix A we list the exact one-photon-exchange amplitudes for the general process $AB \rightarrow AB$.

TABLE I. Hadronic amplitudes involved in interference terms of the most interesting experimental observables.

Observable	Main hadronic amplitudes involved in interference
Proton-proton elastic scattering	
$\frac{d\sigma}{dt}$	$\text{Re}(\Phi_1^N + \Phi_3^N)$
P	$\text{Im}\Phi_2^N$ and $\text{Im}\Phi_5^N$
$A_{NN}; A_{SS}$	$\text{Re}\Phi_2^N$
A_{SL}	$\text{Re}(\Phi_1^N + \Phi_2^N - \Phi_3^N)$
A_{LL}	$\text{Re}(\Phi_1^N - \Phi_3^N)$
$(D_{LL} \sin\theta_R + D_{LS} \cos\theta_R)$	$\text{Re}\Phi_5^N$ and $\text{Re}\Phi_2^N$
$AB \rightarrow AB$; A neutral, B charged	
P_A	σ
P_B	$\text{Im}\Phi_2^N$
A_{SL}	$\text{Re}(\Phi_1^N - \Phi_3^N)$
A_{LS}	$\text{Re}\Phi_2^N$
$(D_{LL}^{(A)} \sin\theta_L - D_{LS}^{(A)} \cos\theta_L)$	
or	$\text{Re}(\Phi_1^N + \Phi_3^N)$
$(D_{LL}^{(A)} \sin\theta_R + D_{LS}^{(A)} \cos\theta_R)$ in the reaction $BA \rightarrow BA$	

The impact-parameter-space transforms of the electromagnetic and hadronic amplitudes are calculated in Appendix B. Appendices C and D summarize the long and complex calculation of the “contaminated” hadronic and “corrected” electromagnetic amplitudes, respectively, in terms of the “pure” hadronic and the one-photon-exchange amplitudes. Complete calculational details and results are available from the authors upon request.

II. THEORETICAL STRUCTURE OF THE ELECTROMAGNETIC-HADRONIC INTERFERENCE

This section is devoted to a general discussion of the theoretical structure of the electromagnetic-hadronic interference terms, and we describe our method of calculating them. For clarity we will initially illustrate our approach for the case of spinless particles.

A. General theoretical approach

At a fundamental level it is clear that combined hadronic and electromagnetic effects should be described by adding together the electromagnetic and hadronic Hamiltonians. However, there is no hope

of utilizing such an approach in practice, and we are forced to look elsewhere for guidance. In the context of nonrelativistic quantum mechanics, it is clear that one should add the Coulomb potential to the hadronic potential appearing in the Schrödinger equation. The ensuing structure is particularly simple and appealing in an eikonal treatment which would be expected to be valid at small scattering angles and high energies. In this case the usual partial-wave amplitude

$$\hat{F}(l) = \frac{e^{2i\delta l} - 1}{2i} \quad (1)$$

is replaced by

$$\hat{F}(b) = \frac{e^{i\chi(b)} - 1}{2i}, \quad (2)$$

where $\chi(b)$, the eikonal, depends on the impact-parameter b related to the angular momentum l by $l = kb$; k is the momentum. The eikonal is simply related to the potential, viz,

$$\chi(\vec{b}) \propto \int_{-\infty}^{+\infty} V(\vec{b}, z) dz, \quad (3)$$

with

$$V = V^{\text{em}} + V^{\text{N}},$$

where V^{em} denotes the electromagnetic (Coulomb) potential and V^{N} is the hadronic or nuclear potential. Thus we obtain

$$\chi(\vec{b}) = \chi^{\text{em}}(\vec{b}) + \chi^{\text{N}}(\vec{b}). \quad (4)$$

For the fixed impact-parameter amplitude $\hat{F}(b)$, one then has

$$\begin{aligned} 2i\hat{F}(b) &= e^{i(\chi^{\text{em}} + \chi^{\text{N}})} - 1 \\ &= [2i\hat{F}^{\text{em}}(b) + 1][2if^{\text{N}}(b) + 1] - 1 \end{aligned} \quad (5)$$

or

$$\hat{F}(b) = \hat{F}^{\text{em}}(b) + f^{\text{N}}(b) + 2i\hat{F}^{\text{em}}(b)f^{\text{N}}(b).$$

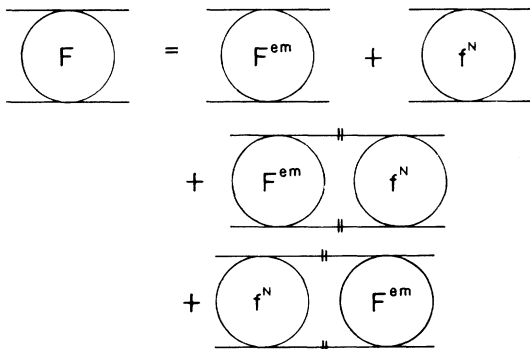


FIG. 1. Relationship between the pure nuclear, electromagnetic, and complete amplitudes in the eikonal approximation. Primed lines are on the mass shell.

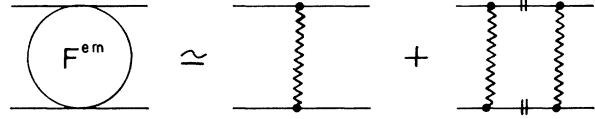


FIG. 2. Expansion of the complete electromagnetic amplitude F^{em} in powers of α .

Here F^{em} and f^{N} are the *complete* electromagnetic and *pure* nuclear amplitudes, respectively. Equation (5), written in a symmetrized form, can be interpreted as the *impact-parameter projection* of the diagrammatic relation given in Fig. 1, where the internal nucleon lines are on the mass shell. The complete electromagnetic amplitude F^{em} can be expanded in powers of α as shown in Fig. 2. To the desired order in α we shall then have the following relation:

$$F = F^{\text{em}} + F^{\text{N}}, \quad (6)$$

where F^{em} is given by Fig. 2 and F^{N} is defined by the diagrams appearing in Fig. 3.

The set of relations appearing in Figs. 1–3, although motivated by an eikonal treatment of nonrelativistic potential theory, transcends its derivation and would seem to offer a very reasonable prescription for calculating electromagnetic-hadronic interference effects, provided, of course, that the diagrams are interpreted as Feynman diagrams. In this context it is important to stress two points:

(i) Although the last two diagrams in Fig. 3 are considered as Feynman diagrams, they are evaluated with the two internal lines on their mass shells. This is not the same as evaluating the imaginary part of the diagram shown in Fig. 4. Indeed the imaginary part would have many other contributions in addition to the contribution given by the two boxlike diagrams in Fig. 3, resulting from also cutting the f^{N} blob in all possible ways.⁸ The prescription we use should be valid at high energies and small momentum transfers.

(ii) Although we have called f^{N} the *pure nuclear* amplitude, it is clear from a more general dia-

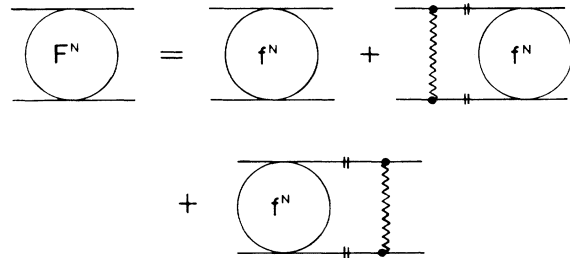


FIG. 3. Definition of the "contaminated" nuclear amplitude F^{N} .

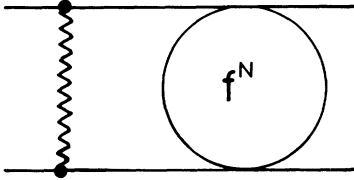


FIG. 4. Feynman-diagram analog of a correction term in F^N .

grammatical point of view that it must include inside itself all manner of electromagnetic contributions. For example, it could contain terms as shown in Fig. 5, in which a photon begins but does not tend on an external line, or is not attached at all to any external lines. As such terms are far beyond our capabilities of calculation at present and will probably remain so for a long time to come, we have no choice but to assume that these effects alter the *pure* nuclear amplitude only marginally. We shall ignore the fact that what we call the "pure nuclear amplitude" f^N is slightly contaminated by electromagnetic effects.

B. Structure of the results in the spinless case

It is well known that the boxlike diagrams appearing in Figs. 2 and 3 diverge as a result of the masslessness of the photon. We formally give the photon a mass λ and we denote by f^{em} the electromagnetic amplitude in the one-photon-exchange approximation, as shown in the middle diagram of Fig. 2 in which allowance is made for a form factor $F_1(q^2)$ ($q^2 = -t$) in the photon-particle coupling. One then finds that (displaying explicitly only terms which are singular as $\lambda \rightarrow 0$) F^{em} and F^N are of the form

$$\begin{aligned} F^{\text{em}} &= [1 + i\alpha F_1^2 \ln\lambda^2 / |t| + O(\alpha)] f^{\text{em}}, \\ F^N &= [1 + i\alpha F_1^2 \ln\lambda^2 + O(\alpha)] f^N, \end{aligned} \quad (7)$$

where F_1 is shorthand for $F_1(q^2=0)$. Correct to the same order in α these can be written as

$$\begin{aligned} F^{\text{em}} &= [\exp(i\alpha F_1^2 \ln\lambda^2)] [1 + O(\alpha)] f^{\text{em}} \exp(-i\alpha F_1^2 \ln|t|), \\ F^N &= [\exp(i\alpha F_1^2 \ln\lambda^2)] [1 + O(\alpha)] f^N, \end{aligned} \quad (8)$$

where $\alpha F_1^2 \ln|t|$ is relevant to the Coulomb phase mentioned in Sec. I. Hence the total amplitude $F = F^{\text{em}} + F^N$ possesses the common phase factor

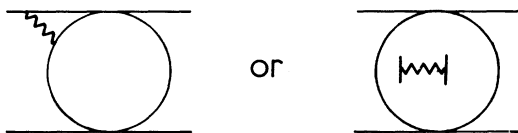


FIG. 5. Examples of electromagnetic corrections not taken into account.

$\exp(i\alpha F_1^2 \ln\lambda^2)$ which then cancels out in the bilinear expression for any physically measurable quantity. A detailed treatment of the infinite-phase problem is given by Yennie, Frautschi, and Suura.⁹ The infinite phase is irrelevant for us and from now on we shall indicate by F^{em} and F^N the amplitude remaining after factoring out the infinite phase.

The terms $O(\alpha)$ in Eq. 8 are all nonsingular in t , so that F^{em} and F^N have basically the same t dependence as $t \rightarrow 0$ as f^{em} and f^N , respectively, aside that is from the explicit $\ln|t|$ term in F^{em} .

A measurement of

$$\frac{d\sigma}{d\Omega} = |F|^2 = |F^{\text{em}} + F^N|^2$$

will therefore show the characteristic interference between F^{em} and F^N . We stress that in principle it is the interference between F^{em} and F^N that is measured directly and not that between f^{em} and f^N as is often stated. It so happens that in the *spinless case* $F^N = f^N$ up to terms of order α and that

$$F^{\text{em}} = f^{\text{em}} \exp(-i\alpha F_1^2 \ln|t|)$$

up to terms of order α^2 , so that aside from the *enhanced* order- α term $\alpha \ln|t|$, the interference is for all practical purposes between f^{em} and f^N .

When we come to deal with the full effects of spin we shall find that there exist other enhanced order- α terms. We shall therefore insist upon the distinction between f^N and F^N . Moreover, we claim that it is really F^N that is measured in normal hadronic experiments even well outside the interference region, e.g., that

$$\frac{d\sigma}{d\Omega} = |F^N|^2,$$

and that σ_{tot} as measured in an attenuation experiment is related to $\text{Im}F^N$ and not $\text{Im}f^N$. Corrections should therefore be applied to F^N to extract from it the nuclear amplitude f^N . These corrections are strictly of order α in the spinless case and are therefore ignored, but as we shall see, this cannot be done in the case of spin- $\frac{1}{2}$ -spin- $\frac{1}{2}$ scattering.

C. General effects of magnetic moment and spin

We now consider the elastic scattering of two spin- $\frac{1}{2}$ particles. We wish to study processes such as $pp \rightarrow pp$, $np \rightarrow np$, and $\Lambda p \rightarrow \Lambda p$. Only the general theoretical structure is discussed here, while the details are confined to the Appendices.

Usually both $pp \rightarrow pp$ and $np \rightarrow np$ are described within the single framework of nucleon-nucleon scattering, by making use of isotopic-spin invariance. The nucleon-nucleon process requires five independent helicity amplitudes for its complete

specification. If, however, we are considering electromagnetic corrections, then, *a priori*, it is clear that we may not invoke invariance under isotopic spin. Consequently, one of the symmetries of the nucleon-nucleon amplitude under the exchange of particles, which is based upon the generalized Pauli principle, no longer holds, and it becomes necessary to use six independent helicity amplitudes for $np \rightarrow np$. Since for $\Lambda p \rightarrow \Lambda p$ it is in any case necessary to use six amplitudes, it will be convenient to divide our treatment into two sections, the first dealing with $p\bar{p} \rightarrow p\bar{p}$ and the second with the process $A+B \rightarrow A+B$, where A and B are nonidentical spin- $\frac{1}{2}$ fermions.

In the spinless case we were able to motivate our approach from the eikonal approximation in

$$\hat{\Phi}_{\lambda'\mu';\lambda\mu}(s, b) = \hat{\Phi}_{\lambda'\mu';\lambda\mu}^{\text{em}}(s, b) + \hat{\Phi}_{\lambda'\mu';\lambda\mu}^{\text{N}}(s, b) + \frac{i}{2} \sum_{\lambda''\mu''} [\hat{\Phi}_{\lambda'\mu';\lambda''\mu''}^{\text{em}}(s, b) \hat{\Phi}_{\lambda''\mu'';\lambda\mu}^{\text{N}}(s, b) + \hat{\Phi}_{\lambda'\mu';\lambda''\mu''}^{\text{N}}(s, b) \hat{\Phi}_{\lambda''\mu'';\lambda\mu}^{\text{em}}(s, b)], \quad (9)$$

where $\hat{\Phi}_{\lambda'\mu';\lambda\mu}(s, b)$ is the fixed-impact-parameter analog of the partial-wave helicity amplitude. In fact, we have

$$\hat{\Phi}_{\lambda'\mu';\lambda\mu}(s, b) \rightarrow \langle \lambda'\mu' | T^J | \lambda\mu \rangle. \quad (10)$$

The factor $\frac{1}{2}$ in (9) occurs because T is defined in terms of the S matrix as in Jacob and Wick¹⁰ by

$$S = 1 + iT. \quad (11)$$

(Note that for the spinless case Jacob and Wick's T^i actually corresponds to twice the usual partial-wave amplitude used in the Schrödinger equation.)

D. Proton-proton scattering

Our five helicity amplitudes are defined analogously to those introduced by Goldberger, Grisaru, MacDowell, and Wong¹¹ except for normalization. We shall take

$$\frac{d\sigma}{dt} = \frac{2\pi}{s(s-4m^2)} (|\Phi_1|^2 + |\Phi_2|^2 + |\Phi_3|^2 + |\Phi_4|^2 + 4|\Phi_5|^2), \quad (12)$$

so that our Φ_i , which are dimensionless, satisfy

$$\Phi_i = \sqrt{s} \phi_i^{\text{GGMW}}, \quad (13)$$

and the optical theorem becomes

$$\text{Im}(\Phi_1 + \Phi_3)|_{t=0} = \frac{[s(s-4m^2)]^{1/2}}{4\pi} \sigma_{\text{tot}}. \quad (14)$$

For each Φ_i we write, in analogy with the spinless case, the following:

$$\Phi_i = \Phi_i^{\text{em}} + \Phi_i^{\text{N}}, \quad (15)$$

potential scattering. In the case of spin- $\frac{1}{2}$ -spin- $\frac{1}{2}$ scattering, there does not exist a simple generalization of the relation (3) between the eikonal and the potential because of the noncommutativity of the different pieces of the spin-dependent potentials. Nevertheless the diagrammatic interpretation of the eikonal results seems so reasonable that we shall simply adopt the same prescription, with due allowance, of course, for the spin degrees of freedom, and evaluate the diagrams using impact-parameter techniques.

In practice, this means that we generalize the symmetrized form of Eq. (5), which is the fixed-impact-parameter projection of the diagrammatic Eqs. given in Fig. 1, and which now read as follows:

where Φ_i^{em} is given by the diagrams like those in Fig. 2, and Φ_i^{N} by the diagrams listed in Fig. 6, where ϕ_i are the *pure* nuclear amplitudes. We shall always refer to the Φ_i^{N} as the "contaminated" nuclear amplitudes.

As in the spinless case we find that for all i , both Φ_i^{em} and Φ_i^{N} pick up infinite phases $i\alpha F_1^2 \ln \lambda^2$. Now $F_1(q^2)$ denotes the Dirac charge form factor defined by the usual expression for the electromagnetic current:

$$\langle p'\lambda' | J_\mu | p\lambda \rangle = e\bar{u}_{\lambda'}(p') \left[F_1(q^2) \gamma_\mu + i q^\nu \sigma_{\nu\mu} \frac{\kappa}{2m} F_2(q^2) \right] u_\lambda(p), \quad (16)$$

with $q = p' - p$, and $\kappa = \mu_p - 1$ the anomalous magnetic moment of the proton. The infinite phase is again irrelevant and will be ignored, so that Φ_i^{em} and Φ_i^{N} represent what is left after factoring it out.

If Φ_i^{em} denotes the *one-photon approximation* to the electromagnetic interaction, then we find for all i that

$$\Phi_i^{\text{em}} = [1 + O(\alpha)] \phi_i^{\text{em}} \exp(-i\alpha F_1^2 \ln |t|). \quad (17)$$

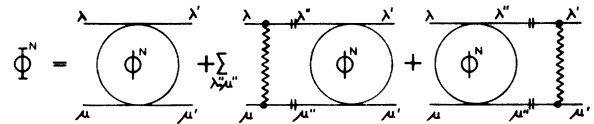


FIG. 6. Definition of the "contaminated" nuclear amplitudes for spin- $\frac{1}{2}$ particles.

The corrections of order $O(\alpha)$ are given for completeness in Appendix D. They are, however, unenhanced and may therefore be neglected. We thus use

$$\Phi_i^{\text{em}} = [\exp(-i\alpha \ln|t|)] \phi_i^{\text{em}}, \quad (i=1, \dots, 5). \quad (18)$$

It should be noted that the Coulomb phase is indeed independent of i as expected from the intuitive discussion in Sec. I.

For the corrected nuclear amplitudes it is simpler to state our results if we first exhibit explicitly the inherent kinematic factors in some of the amplitudes, after removing a factor s for convenience: For $i=1, 2, 3$ we put

$$\Phi_i^{\text{N}}(s, t) = s[C_i(s, t) + iA_i(s, t)];$$

For $i=4$ we put

$$\Phi_4(s, t) = \frac{-ts}{m^2} [C_4(s, t) + iA_4(s, t)]; \quad (19)$$

and for $i=5$ we put

$$\Phi_5(s, t) = \frac{(-t)^{1/2}s}{m} [C_5(s, t) + iA_5(s, t)].$$

The C_i, A_i for all i are in general smooth and nonzero at $t=0$.

For the *pure* nuclear amplitudes we define analogously as follows:

$$\phi_i^{\text{N}}(s, t) = s[c_i(s, t) + ia_i(s, t)], \quad i=1, 2, 3$$

$$\phi_4^{\text{N}}(s, t) = \frac{-ts}{m^2} [c_4(s, t) + ia_4(s, t)], \quad (20)$$

$$\phi_5^{\text{N}}(s, t) = \frac{(-t)^{1/2}s}{m} [c_5(s, t) + ia_5(s, t)].$$

We then find that for all i we obtain

$$C_i(s, t) = c_i(s, t) - \alpha \delta_i(s, t), \quad (21)$$

$$A_i(s, t) = a_i(s, t) + \alpha \epsilon_i(s, t).$$

As there are sums over spins involved in the evaluation of the diagrams shown in Fig. 6, the δ_i, ϵ_i for a given i depend upon the a_j and c_j for *all* j . In fact one has

$$\delta_i(s, t) = M_{ij} a_j(s, t), \quad (22)$$

$$\epsilon_i(s, t) = \bar{M}_{ij} c_j(s, t),$$

where M_{ij}, \bar{M}_{ij} are 5×5 matrices that are smooth functions of t . The exact results for δ_i, ϵ_i are given in Appendix C.

Since in proton-proton scattering some amplitudes are much larger than others, it can easily happen that a *nondiagonal* correction to a small amplitude, although multiplied by α , can be of considerable significance. Such terms are regarded as new *enhanced order- α terms*.

Just as in the spinless case it is really the "con-

taminated" nuclear amplitude Φ_i^{N} that are measured both in normal hadronic experiments and in specifically interference type experiments. In Sec. III we present detailed formulas for all the interesting experimental quantities in the interference region.

E. Scattering of nonidentical spin- $\frac{1}{2}$ particles

In nucleon-nucleon scattering the amplitude Φ_5 corresponds to the helicity transition $\langle ++ | -+ \rangle$. We can consider a sixth amplitude Φ_6 corresponding to the transition $\langle ++ | -+ \rangle$. When the particles are identical, one can show that for the partial-wave helicity amplitudes

$$\langle ++ | T^J | -+ \rangle = \langle ++ | T^J | -+ \rangle \quad (23)$$

as a result of the generalized Pauli principle.

Using the properties of the $d_{\lambda\mu}^j(\theta)$ functions it follows from Eq. (23) that for nucleon-nucleon scattering, if isospin is conserved,

$$\Phi_6(s, t) = -\Phi_5(s, t). \quad (24)$$

When the particles are strictly nonidentical or if in $np \rightarrow np$ isospin is not conserved, we are forced to include Φ_6 as an independent amplitude.

The expression for $d\sigma/dt$ becomes

$$\begin{aligned} \frac{d\sigma}{dt} = \frac{2\pi}{(s-\Delta^2)(s-\Sigma^2)} & (|\Phi_1|^2 + |\Phi_2|^2 + |\Phi_3|^2 \\ & + |\Phi_4|^2 + 2|\Phi_5|^2 + 2|\Phi_6|^2), \end{aligned} \quad (25)$$

where $\Delta = m_A - m_B$ and $\Sigma = m_A + m_B$.

The general expressions for the experimental observables for a process $A+B \rightarrow A+B$, $A \neq B$, are not well known. We present in Sec. III D the formulas for the most important observables.

In calculating the Φ_i^{em} and Φ_i^{N} in terms of ϕ_i^{em} and ϕ_i^{N} , respectively, it is essential to use the correct and indeed totally different expressions for ϕ_5^{em} and ϕ_5^{N} . However, when calculating the diagrams shown in Fig. 6 for $np \rightarrow np$ it is sufficient to put $\phi_5^{\text{N}} = -\phi_5^{\text{N}}$ inside the diagram, since in this case ϕ_5^{N} will differ from $-\phi_5^{\text{N}}$ by terms of order α only.

The structure of the results for the general process $A+B \rightarrow A+B$ is essentially the same as in the $pp \rightarrow pp$ case. There emerges an infinite phase $i\alpha F_1^A F_1^B \ln \lambda^2$ and a Coulomb phase $i\alpha F_1^A F_1^B \ln|t|$, which are the same in each of the six amplitudes. Here F_1^A, F_1^B are the Dirac form factors for particles A and B , respectively, evaluated at $q^2=0$. In the event that one of the particles, say A is uncharged, we would have $F_1^A=0$ and both the infinite phase and the Coulomb phase would disappear. There will, nonetheless, still be *enhanced order- α corrections* as a result of the spin structure.

If we slightly modify and extend the definitions

(19), (20), and (21) by the replacements

$$\begin{aligned}\Phi_5^N(s, t) &= \frac{(-t)^{1/2} S}{m_B} [C_5(s, t) + iA_5(s, t)], \\ \phi_5^N(s, t) &= \frac{(-t)^{1/2} S}{m_B} [c_5(s, t) + i a_5(s, t)], \\ \Phi_4^N(s, t) &= \frac{-tS}{m_A m_B} [C_4(s, t) + iA_4(s, t)], \\ \phi_4^N(s, t) &= \frac{-tS}{m_A m_B} [c_4(s, t) + i a_4(s, t)],\end{aligned}\quad (26)$$

and we include the new amplitudes

$$\begin{aligned}\Phi_6^N(s, t) &= \frac{S(-t)^{1/2}}{m_A} [C_6(s, t) + iA_6(s, t)], \\ \phi_6^N(s, t) &= \frac{S(-t)^{1/2}}{m_A} [c_6(s, t) + i a_6(s, t)],\end{aligned}\quad (27)$$

then we find, in addition to (21), that

$$\begin{aligned}C_6(s, t) &= c_6(s, t) - \alpha \delta_6(s, t), \\ A_6(s, t) &= a_6(s, t) + \alpha \epsilon_6(s, t),\end{aligned}$$

and the δ_i , ϵ_i are now given in terms of the a_j , c_j by 6×6 matrices M_{ij} , \bar{M}_{ij} analogous to (22).

Note that if $A \equiv B$ we will have $C_6(s, t) = -C_5(s, t)$, etc. In Sec. III we give formulas valid in the interference region for all the experimental quantities of interest for the reactions $np \rightarrow np$ and $\Lambda p \rightarrow \Lambda p$.

III. PHENOMENOLOGICAL STRUCTURE OF THE INTERFERENCE

In this section we first discuss the general structure of the interesting experimental observables in the interference region. We then provide a detailed list of those observables which might become accessible to measurement at small t in the near future, and consider what information concerning the hadronic amplitudes, can be extracted from them.

As mentioned earlier the interference really occurs between the *corrected* electromagnetic amplitudes Φ_i^{em} and the “contaminated” nuclear amplitudes Φ_i^N . Thus the experimental measurements give information most directly about the “contaminated” nuclear amplitudes Φ_i^N . It is therefore simpler to break up our study of the *pure* nuclear amplitudes into two steps:

- (i) experiment \rightarrow “contaminated” nuclear amplitude Φ_i^N ;
- (ii) “contaminated” nuclear amplitude $\Phi_i^N \rightarrow$ “pure” nuclear amplitude ϕ_i^N .

In this section we shall be concerned solely with point (i), i.e., with the extraction of the “contaminated” nuclear amplitudes from the ex-

perimental measurements. Point (ii) is discussed in Sec. IV.

A. The general structure in proton-proton scattering

The interference region for proton-proton scattering is defined roughly by the requirement $|t| \lesssim \alpha$ (GeV/c)², i.e., $|t| \lesssim 0.01$ (GeV/c)².

If we denote by X a typical experimental observable

$$\left(\frac{d\sigma}{dt}, P \frac{d\sigma}{dt}, C_{NN} \frac{d\sigma}{dt}, \dots \right),$$

we find that generally the structure it can have for small t is

$$X(t) = \frac{\alpha^2 X^{(2)}}{t^2} + \frac{\alpha}{t} [X^{(1)} - \alpha \bar{X}^{(1)} \ln] + X^{(0)} + X^{(0)'} t, \quad (28)$$

where all the coefficients $X^{(i)}$, $\bar{X}^{(i)}$ are independent of t . Note that Eq. (28) is also valid well outside the interference region.

The coefficient $X^{(2)}$ is given purely by electromagnetic effects and depends only on the charges of the particles and on the observables under study. Naturally, not all observables are as singular as $1/t^2$ for small t .

In principle, if the data were accurate enough, we could hope to extract all the coefficients $X^{(i)}$, $\bar{X}^{(i)}$ in Eq. (28), from a fit to the experimental points in the interference region. In some cases the fit could be complemented by the fact that one or more of the coefficients are known or approximately known from other sources, e.g., from total-cross-section measurements, etc.

In practice it is most unlikely that all the coefficients can be well determined from measurements in the interference region, and we must consider how to supplement information from this region in a consistent fashion. When $X(t)$ is measured over a wide range of t spanning both the interference region $|t| \lesssim \alpha$ and the “usual small- t ” region, say $m^2 \gg |t| \gg \alpha$, it might be preferable to do separate fits to the two regions.

In the “usual small- t ” region one would put

$$X(t) = X^{(0)} + X^{(0)'} t, \quad (29)$$

and thus determine the parameters $X^{(0)}$ and $X^{(0)'}$. With these known and fixed, one could then proceed to determine the parameters $X^{(1)}$, $\bar{X}^{(1)}$ using (28) in the interference region. Should the interference-region fit still fail to reasonably fix the parameters, it would be necessary to ignore the t variation of the $\ln|t|$ term in (28). One could then attempt to fit the interference region using

$$X(t) = \frac{\alpha^2 X^{(2)}}{t^2} + \frac{\alpha \bar{X}^{(1)}}{t} + X^{(0)}, \quad (30)$$

and the average coefficients $\bar{X}^{(1)}$ would be given approximately by

$$\bar{X}^{(1)} = X^{(1)} - \alpha \bar{X}^{(1)} \ln|\bar{t}|, \quad (31)$$

where $\ln|\bar{t}|$ is the mean value of $\ln|t|$ over the region of the fit. [If this region is defined by $|t|_{\min} \leq |t| \leq |t|_{\max}$ then $|\bar{t}| = (|t|_{\min}|t|_{\max})^{1/2}$.]

In what follows we shall assume that $X^{(0)}$ and $X^{(0)'}$ have been determined from measurements in the "usual small t " region. We shall also usually assume that the coefficients $X^{(1)}$, $\bar{X}^{(1)}$ can be determined from the interference region, and shall be concerned with relating these coefficients to the "contaminated" nuclear amplitudes.

In general the coefficients are given by a mixture of hadronic and electromagnetic contributions. For example,

$$X^{(0)} = X^N + \alpha Y^{(0)}, \quad (32)$$

where X^N is the observable $X(t)$ evaluated at $t=0$ using only the "contaminated" nuclear amplitudes, and $Y^{(0)}$ is a quantity of hadronic magnitude. If the observable $X(t)$ has a typical hadronic magnitude and if we plan to work to an accuracy of 5–10% then we can clearly neglect the $O(\alpha)$ term. Indeed, up to the present, fits of type (29) to the "usual small- t " region have always been interpreted as giving directly the hadronic contribution X^N to $X(t)$. However, it seems very likely (as is indicated by the very small proton-proton polarization found at Fermilab¹²) that at high energies some observables will be extremely small, on a hadronic scale. When this is so, it can happen that the coefficient $Y^{(0)}$ in Eq. (32) is so much larger than X^N that the $Y^{(0)}$ term is crucial in interpreting the measured value of $X^{(0)}$. We shall demonstrate this phenomenon in the case of the polarization and the spin-correlation parameter C_{NN} in proton-proton scattering. We emphasize that although these effects are electromagnetic, they are not the usual interference effects and they also influence the measurements *completely outside the interference region*. We now turn to a detailed consideration of the interference effects.

B. Parametrization of the amplitudes

To the accuracy required, we have the following for all i for the process $A+B \rightarrow A+B$:

$$\Phi_i^{\text{em}} = \phi_i^{\text{em}} \exp(-i \alpha F_1^A F_1^B \ln|t|). \quad (33)$$

The one-photon amplitudes ϕ_i^{em} are given exactly in Appendix A. We are only interested in their *leading terms at high energies*; these are, with $t = -q^2$,

$$\phi_1^{\text{em}} = \phi_3^{\text{em}} = \frac{\alpha S}{t} F_1^A(-t) F_1^B(-t), \quad (34)$$

$$\phi_2^{\text{em}} = -\phi_4^{\text{em}} = \frac{\alpha S \kappa_A \kappa_B}{4m_A m_B} F_2^A(-t) F_2^B(-t),$$

$$\phi_5^{\text{em}} = \frac{-\alpha S}{(-t)^{1/2}} \frac{\kappa_B}{2m_B} F_1^A(-t) F_2^B(-t), \quad (35)$$

$$\phi_6^{\text{em}} = \frac{\alpha S}{\sqrt{(-t)^{1/2}}} \frac{\kappa_A}{2m_A} F_1^B(-t) F_2^A(-t), \quad (36)$$

where κ refers to the *anomalous* magnetic moment of the particles, and $F_1(q^2)$, $F_2(q^2)$ are the Dirac form factors. The form factors are normalized to 1 at $q^2=0$ unless they actually vanish at this point, and the signs in Eqs. (34)–(36) correspond to positively-charged particles. Two important points should be noted:

(i) For $pp \rightarrow pp$ we have $A=B$ and we simply ignore ϕ_6^{em} . The amplitudes ϕ_1^{em} , ϕ_3^{em} , and ϕ_5^{em} are all singular as $t \rightarrow 0$.

(ii) If one particle is neutral as in $\Lambda p \rightarrow \Lambda p$ and $n p \rightarrow n p$ we have $F_1^A(0) = 0$. In this case we put

$$F_1^A(q^2) = q^2 \bar{F}_1^A(q^2), \quad (37)$$

and we see that neither ϕ_5^{em} nor ϕ_1^{em} nor ϕ_3^{em} are singular as $t \rightarrow 0$. In this case only ϕ_6^{em} remains singular as $t \rightarrow 0$.

For very small t we parameterize the form factors as

$$F_1^A(q^2) = F_1^A \exp(-\beta_1^A q^2), \quad (38)$$

$$F_2^A(q^2) = F_2^A \exp(-\beta_2^A q^2).$$

When, for example, $F_1^A(0) = F_1^A = 0$ we use

$$\bar{F}_1^A(q^2) = \bar{F}_1^A \exp(-\beta_1^A q^2). \quad (39)$$

In practice, we are only interested in the first two terms in the expansion about $q^2=0$; thus the exponential forms are not to be taken seriously.

For the "contaminated" nuclear amplitudes Φ_1^N we have already introduced a parametrization in terms of $C_i(s, t)$, $A_i(s, t)$ [see Eqs. (19) and (26)] which exposes essential kinematic factors. We now write the following;

$$A_i(s, t) = A_i \exp(\bar{b}_i t), \quad (40)$$

$$C_i(s, t) = C_i \exp(\bar{c}_i t),$$

in which we allow for a possible difference of slope of the real and imaginary parts.

In terms of A_i ; the optical theorems become

$$\begin{aligned} \sigma_{\text{tot}} &= 4\pi(A_1 + A_3), \\ \Delta\sigma_T &= \sigma_{\uparrow\uparrow} - \sigma_{\uparrow\downarrow} = -8\pi A_2, \\ \Delta\sigma_L &= \sigma_{\uparrow\uparrow} - \sigma_{\uparrow\downarrow} = 8\pi(A_1 - A_3), \\ \sigma_{\uparrow\uparrow} &= 4\pi(A_1 + A_2 + A_3), \end{aligned} \quad (41)$$

where the latter three cross sections refer to the initial protons being in definite spin states.¹³

C. Interference measurements in proton-proton scattering

We list those experimental observables which show interesting structure in the interference region and we indicate which "contaminated" nuclear amplitudes are probed by a measurement of the interference terms. Electromagnetic quantities without labels in this section of course refer to the proton.

(i) The spin-averaged invariant differential cross section provides a knowledge of the $\text{Re}(\Phi_1^N + \Phi_3^N)$ at $t=0$. For one has that

$$I \equiv \frac{d\sigma}{dt} = \frac{2\pi}{s(s-4m^2)} (|\Phi_1|^2 + |\Phi_2|^2 + |\Phi_3|^2 + |\Phi_4|^2 + 4|\Phi_5|^2) \\ = 4\pi \left[\frac{\alpha^2}{t^2} + \frac{\alpha}{t} (I^{(1)} - \alpha \bar{I}^{(1)} \ln|t|) + I^{(0)} \right], \quad (42)$$

where, correct to $O(\alpha)$, the coefficients are given in terms of the "contaminated" nuclear amplitudes as follows:

$$I^{(1)} = C_1 + C_3 + \alpha \left(4\beta_1 - \frac{\kappa_p^2}{2m^2} \right), \quad (43)$$

$$\bar{I}^{(1)} = A_1 + A_3 = \frac{\sigma_{\text{tot}}}{4\pi}, \quad (44)$$

with σ_{tot} measured in $(\text{GeV}/c)^{-2}$, and

$$I^{(0)} = \frac{1}{4\pi} \left. \frac{d\sigma^N}{dt} \right|_{t=0} \\ + \alpha \left[C_1(2\beta_1 + \bar{b}_1) + C_3(2\beta_1 + \bar{b}_3) + \frac{\kappa_p^2}{4m^2} (C_2 - 8C_5) \right] \quad (45)$$

in which $d\sigma^N/dt$ is the expression for $d\sigma/dt$ obtained using the "contaminated" nuclear amplitudes Φ_i^N . Thus we arrive at

$$\frac{1}{4\pi} \left. \frac{d\sigma^N}{dt} \right|_{t=0} = \left(\frac{\sigma_T}{8\pi} \right)^2 (1 + \rho^2) + \frac{1}{4} (C_1 - C_3)^2 \\ + \frac{1}{4} (A_1 - A_3)^2 + \frac{1}{2} (C_2^2 + A_2^2), \quad (46)$$

where as usual

$$\rho \equiv \frac{\text{Re}(\Phi_1^N + \Phi_3^N)}{\text{Im}(\Phi_1^N + \Phi_3^N)} \Big|_{t=0} = \frac{C_1 + C_3}{A_1 + A_3}. \quad (47)$$

Since β_1 and κ_p are known, Eq. (43) allows the evaluation of $C_1 + C_3$ or ρ . The $O(\alpha)$ corrections in (43) are negligible unless it happens that ρ is very small, as is indeed the case at Fermilab energies.

In Eq. (45) the corrections are negligible, given that $d\sigma^N/dt$ is dominated by the imaginary parts of the nonflip amplitudes. Thus $I^{(0)}$ gives the

value of $d\sigma^N/dt$ at $t=0$ to a high degree of accuracy. However, it would be meaningless to use the value of $I^{(0)}$ to probe *very* small helicity-flip amplitudes while neglecting the $O(\alpha)$ corrections in (46).

(ii) The polarization gives a great deal of information about the helicity-flip amplitudes near $t=0$. We have

$$P \frac{d\sigma}{dt} = \frac{-4\pi}{s(s-4m^2)} \text{Im}[\Phi_5^* (\Phi_1 + \Phi_2 + \Phi_3 - \Phi_4)], \quad (48)$$

and we find that

$$\frac{m}{(-t)^{1/2}} P \frac{d\sigma}{dt} = 4\pi \left[\frac{\alpha}{t} (B^{(1)} - \alpha \bar{B}^{(1)} \ln|t|) + B^{(0)} \right]. \quad (49)$$

The B^i are given to $O(\alpha)$ in terms of the "contaminated" nuclear amplitudes as follows:

$$B^{(1)} = 2A_5 - \frac{\kappa_p}{8\pi} \sigma_{\uparrow\uparrow}, \quad (50)$$

where $\sigma_{\uparrow\uparrow}$ is the total cross section for the collision of protons polarized perpendicular to the reaction plane.

$$\bar{B}^{(1)} = \frac{\kappa_p}{2} (C_1 + C_2 + C_3) - 2C_5, \quad (51)$$

$$B^{(0)} = \frac{1}{4\pi} \left[\frac{m}{(-t)^{1/2}} P \frac{d\sigma}{dt} \right]_{t=0}^N \\ - \alpha \left[\frac{\kappa_p}{8\pi} \sigma_{\uparrow\uparrow} (\beta_1 + \beta_2) \right. \\ \left. + \frac{\kappa_p}{2} \left(A_1 b_1 + A_2 b_2 + A_3 b_3 + \frac{A_4}{m^2} \right) \right. \\ \left. - 2A_5 \left(2\beta_1 + b_5 + \frac{\kappa_p^2}{4m^2} \right) \right], \quad (52)$$

in which

$$\frac{1}{4\pi} \left[\frac{m}{(-t)^{1/2}} P \frac{d\sigma}{dt} \right]_{t=0}^N = A_5 (C_1 + C_2 + C_3) \\ - C_5 (A_1 + A_2 + A_3). \quad (53)$$

In the event that $\sigma_{\uparrow\uparrow}$ is not measured, it can be replaced in (50) by

$$\sigma_{\uparrow\uparrow} = 4\pi A_2 + \sigma_{\text{tot}}. \quad (54)$$

We assume that $B^{(0)}$ is known from the "usual small- t " region measurements. If then $\bar{B}^{(1)}$ and $B^{(1)}$ could be determined from the data, they would provide two equations for the four unknowns A_2, A_5, C_2, C_5 .

However, since real parts are expected to be fairly small at high energies, it is unlikely that the $\bar{B}^{(1)}$ terms can be determined from the t dependence of the data. But, this does not mean that one can simply neglect this term. In very many high-energy models one would expect A_5

$\ll C_5$ in proton-proton scattering (e.g., $A_5 = 0$ in exchange-degenerate Regge models) so that the enhanced contribution $\alpha \bar{B}^{(1)} \ln|t|$ could easily be as large as the contribution of A_5 to $B^{(1)}$.

In practice then, one should try to disentangle $B^{(1)}$ and $\bar{B}^{(1)}$ from the data. If, however, this provides impossible, it might be advisable to find the overall coefficient of $4\pi\alpha/t$, call it $\bar{B}^{(1)}$, and to interpret this using the mean value of $\ln|t|$ over the region of the data fit. Thus we might use

$$\bar{B}^{(1)} = B^{(1)} - \alpha \bar{B}^{(1)} \ln|\bar{t}| \quad (55)$$

as discussed in Sec. III A.

In this case, $C_1 + C_3$ is known from $d\sigma/dt$ interference measurements; $\bar{B}^{(1)}$ provides only one equation for the real and imaginary parts of Φ_2^N and Φ_5^N .

The known value of $B^{(0)}$ can provide us with a further equation for the hadronic amplitudes, but care must be taken with the $O(\alpha)$ corrections in Eq. (52).

Indeed, if P is fairly small, say less than 10% at $t = -0.1$, then the $O(\alpha)$ corrections in Eq. (52) are substantial and it would be quite incorrect to take the measured $B^{(0)}$ as the value of $(1/4\pi) [m/(-t)^{1/2}] (P d\sigma/dt)^N$ at $t=0$.

To estimate the importance of the $O(\alpha)$ corrections in Eq. (52), we may put $A_1 = A_3$, $b_1 = b_3 = b$, where $2b$ is the logarithmic slope of $d\sigma^N/dt$ at $t=0$, and neglect A_4 .

Then we obtain

$$B^{(0)} \approx \frac{1}{4\pi} \frac{m}{(-t)^{1/2}} \left(P \frac{d\sigma}{dt} \right)_{t=0}^N - \frac{\alpha \kappa_p}{8\pi} \sigma_{\text{tot}} (\beta_1 + \beta_2 + b). \quad (56)$$

If we approximate $d\sigma^N/dt$ at $t=0$ by its optical value $\sigma_T^2/16\pi$ we obtain

$$B^{(0)} = \frac{\sigma_{\text{tot}}}{64\pi^2} \left\{ \frac{m}{(-t)^{1/2}} P^N \sigma_{\text{tot}} - 8\pi \alpha \kappa_p (\beta_1 + \beta_2 + b) \right\}. \quad (57)$$

Using $\kappa_p \sim 1.8$, $2b \sim 10$, $\sigma_T \sim 100$ (GeV/c) $^{-2}$, $\beta_1 + \beta_2 \sim 7.8$ and putting $P^N = [(-t)^{1/2}/m] \mathcal{P}$ for small t , the curly bracket becomes roughly $100\mathcal{P} - 4$. If P^N is of the order of 6% or less at $t = -0.1$ then $\mathcal{P} \leq 18\%$ and the correction terms are sizable, $\approx 25\%$.

Because the $O(\alpha)$ terms are relatively large in (52), the contribution to the polarization coming from electromagnetically induced spin flip could be of importance at Fermilab energies, even outside the interference region.¹⁴

To illustrate this, we have calculated the polarization produced electromagnetically when the

hadronic polarization is actually zero. In this calculation we used the exact one-photon-exchange electromagnetic amplitudes (Appendix A) rather than their expansion for small t in order to be able to reach reasonably large values of t . For the hadronic amplitudes we put $\Phi_2^N = \Phi_4^N = \Phi_5^N = 0$, and $\Phi_1^N = \Phi_3^N$ was obtained from the dispersion theoretic analysis of Grein, Guigas, and Kroll.¹⁵ The values used for $\Phi_1^N = \Phi_3^N$ provide an excellent fit to the pp $d\sigma/dt$ over a range of $0 \leq -t < 0.7$ (GeV/c) 2 .

The results of our calculation are shown in Fig. 7 where P is plotted for several values of the energy. It is seen from this figure that measured values of $P \leq 3\%$, as reported from Fermilab must not be interpreted literally as the values of the hadronic polarization.

Returning to the problem of determining the hadronic amplitudes, we see that Eq. (56), together with Eq. (53) provides one further constraint on Φ_2^N and Φ_5^N .

To summarize, a determination of all the coefficients $B^{(1)}$, $\bar{B}^{(1)}$, $B^{(0)}$ would, to a good approximation, provide three equations for A_2 , C_2 , A_5 , C_5 . More realistically, a knowledge of just $\bar{B}^{(1)}$ and $B^{(0)}$ will provide two equations for the four amplitudes.

(iii) The spin-correlation parameter A_{NN} ($= C_{NN}$) provides information on $\text{Re } \Phi_2^N$ at $t=0$. This is of great interest since the isotopic spin-1 exchange contribution to $\text{Re } \Phi_2^N$ is supposed to be well known from studies of neutron-proton charge-exchange scattering. It is often conceived that the isospin-0 exchange contribution to $\text{Re } \Phi_2^N$ is negligible. If this is so, then the value of $\text{Re } \Phi_2^N$ in $pp \rightarrow pp$ is known from its value in $np \rightarrow pn$. A direct measurement of $\text{Re } \Phi_2^N$ in $pp \rightarrow pp$ is therefore of great value.

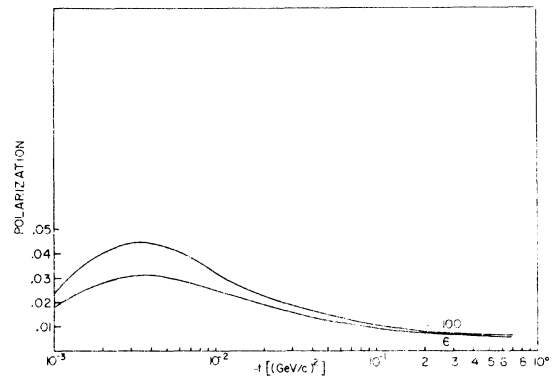


FIG. 7. Electromagnetically induced polarization in proton-proton scattering at laboratory momenta of 6 and 100 GeV/c.

One has⁽¹⁶⁾

$$\begin{aligned} A_{NN} \frac{d\sigma}{dt} &= I(N, N; 0, 0) \\ &= \frac{4\pi}{s(s-4m^2)} [\operatorname{Re}(\Phi_1^* \Phi_2 - \Phi_3^* \Phi_4) + 2|\Phi_5|^2] \\ &= 4\pi \left[\frac{\alpha}{t} (D^{(1)} - \alpha \bar{D}^{(1)} \ln|t|) + D^{(0)} \right], \end{aligned} \quad (58)$$

where

$$D^{(1)} = C_2 \quad (59)$$

$$\bar{D}^{(1)} = A_2 = -\frac{\Delta\sigma_T}{8\pi} \quad (60)$$

$$\begin{aligned} D^{(0)} &= \frac{1}{4\pi} \left(A_{NN} \frac{d\sigma}{dt} \right)_{t=0}^N + \alpha \left[\frac{\kappa_p^2}{4m^2} (C_1 + C_3) + C_2(2\beta_1 + \bar{b}_2) \right. \\ &\quad \left. - \frac{2\kappa_p}{m} C_5 + \frac{C_4}{m^2} \right], \end{aligned} \quad (61)$$

and in which we have

$$\frac{1}{4\pi} \left(A_{NN} \frac{d\sigma}{dt} \right)_{t=0}^N = C_1 C_2 + A_1 A_2. \quad (62)$$

As usual, we assume $D^{(0)}$ known from measurements in the “usual small- t ” region. If the other coefficients $D^{(1)}$ and $\bar{D}^{(1)}$ can be fixed in the interference region, then an enormous amount of information becomes available.

Eqs. (59) and (60) give the real and imaginary parts of Φ_2^N directly.

Turning now to $D^{(0)}$, we see from (61) that it is unlikely that the $O(\alpha)$ correction terms will be important at high energies unless A_{NN} is exceedingly small, say $\approx 1\%$. Nevertheless, the terms most likely to be important in Eq. (61) are those involving C_1 , C_3 and C_2 which should be incorporated, with a reasonable guess at the slope \bar{b}_2 , in the extraction of $A_{NN} d\sigma^N/dt$ at $t=0$ from the measurement value of $D^{(0)}$.

At low energies, where ρ is not so small, the *electromagnetically induced* A_{NN} is surprisingly large outside the interference region. Using the method described in subsection (ii) above, we have calculated A_{NN} for a range of energies as shown in Fig. 8. These values are not small compared with measured values of A_{NN} at 6 and 12 GeV/c at $t \approx -0.1$, which suggests that some care is necessary in interpreting the usual A_{NN} measurements.

In practice, a realistic strategy might involve neglecting C_4 , C_5 in Eq. (61), putting $A_1 \approx A_3$, $C_1 \approx C_3$ so that both A_1 and C_1 are then known, and then doing the interference fit and a fit to the known $D^{(0)}$ in terms of just the two parameters A_2 and C_2 .

In Sec. IV we shall see that even when the “con-

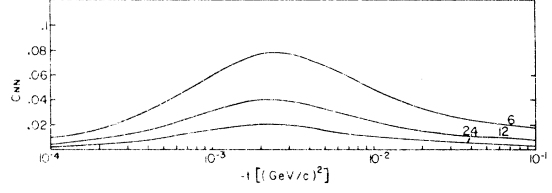


FIG. 8. Electromagnetically induced spin correlation parameter C_{NN} at $p_{\text{lab}} = 6, 12,$ and 24 GeV/c.

taminated” nuclear amplitudes have been extracted from the data, there may be quite substantial corrections involved in extracting the “pure” hadronic amplitude ϕ_2^N from Φ_2^N .

(iv) The correlation parameter A_{SS} gives essentially the same type of information as A_{NN} does, although Φ_5 no longer participates.

We have

$$\begin{aligned} A_{SS} \frac{d\sigma}{dt} &= I(S, S; 0, 0) \\ &= \frac{4\pi}{s(s-4m^2)} \operatorname{Re}(\Phi_1^* \Phi_2 + \Phi_3^* \Phi_4) \\ &= 4\pi \left[\frac{\alpha}{t} (D^{(1)} - \alpha \bar{D}^{(1)} \ln|t|) + E^{(0)} \right], \end{aligned} \quad (63)$$

where $D^{(1)}$ and $\bar{D}^{(1)}$ are the same as written in Eqs. (59) and (60), but

$$\begin{aligned} E^{(0)} &= \frac{1}{4\pi} \left(A_{NN} \frac{d\sigma}{dt} \right)_{t=0}^N \\ &\quad + \alpha \left[\frac{\kappa_p^2}{4m^2} (C_1 - C_3) + C_2(2\beta_2 + \bar{b}_2) - \frac{C_4}{m^2} \right]. \end{aligned} \quad (64)$$

In (64) we have used the fact that $A_{NN} = A_{SS}$ at $t=0$.

Essentially the same comments apply to A_{SS} as were made about A_{NN} in subsection (iii) above.

(v) The correlation parameter A_{SL} determines the real part of $\Phi_1^N + \Phi_2^N - \Phi_3^N$. Assuming that $\operatorname{Re}\Phi_2^N$ is known from subsections (iii) or (iv) we derive information about the differences between the real parts of the nonflip amplitudes Φ_1^N and Φ_3^N . It has long been taken for granted that $\Phi_1^N = \Phi_3^N$, but recent measurements⁽¹⁷⁾ of $\Delta\sigma_L = \sigma_{\rightarrow\rightarrow} - \sigma_{\rightarrow\leftarrow}$ which depend upon $\operatorname{Im}\Phi_1^N - \operatorname{Im}\Phi_3^N$ have yielded amazingly large values at moderate energies. A check on the real parts is therefore of great interest.

One has

$$\begin{aligned} A_{SL} \frac{d\sigma}{dt} &= I(S, L; 0, 0) \\ &= \frac{4\pi}{s(s-4m^2)} \operatorname{Re}[\Phi_5^*(\Phi_1 + \Phi_2 - \Phi_3 + \Phi_4)] \end{aligned} \quad (65)$$

and finds

$$\frac{m}{(-t)^{1/2}} A_{SL} \frac{d\sigma}{dt} = 4\pi \left[\frac{\alpha}{t} (G^{(1)} - \alpha \bar{G}^{(1)} \ln|t|) + G^{(0)} \right] \quad (66)$$

where,

$$G^{(1)} = \frac{\kappa_p}{2} (C_1 + C_2 - C_3), \quad (67)$$

$$\bar{G}^{(1)} = \frac{\kappa_p}{2} (A_1 + A_2 - A_3), \quad (68)$$

and,

$$G^{(0)} = \frac{1}{4\pi} \frac{m}{(-t)^{1/2}} \left(C_{SL} \frac{d\sigma}{dt} \right)_{t=0}^N + \frac{\alpha \kappa_p}{2} \left[C_1 \bar{b}_1 + C_2 \bar{b}_2 - C_3 \bar{b}_3 + (C_1 + C_2 - C_3)(\beta_1 + \beta_2) - \frac{C_4}{m^2} \right]. \quad (69)$$

Here

$$\frac{1}{4\pi} \frac{m}{(-t)^{1/2}} \left(A_{SL} \frac{d\sigma}{dt} \right)_{t=0}^N = C_5 (C_1 + C_2 - C_3) + A_5 (A_1 + A_2 - A_3) - \frac{2}{\kappa_p} [C_5 G^{(1)} + A_5 \bar{G}^{(1)}]. \quad (70)$$

Assuming $G^{(0)}$, known from the "usual small- t " measurements, a determination of $G^{(1)}$ and $\bar{G}^{(1)}$ immediately gives the value of $C_1 - C_3$ and $A_1 - A_3$. If total-cross-section measurements for protons in definite longitudinal spin states are available, then $\bar{G}^{(1)}$ is fixed by

$$\bar{G}^{(1)} = \frac{\kappa_p}{2} \left(A_2 + \frac{\Delta\sigma_L}{8\pi} \right). \quad (71)$$

In Eq. (69) one might attempt to neglect C_4 and to take $\bar{b}_1 \approx \bar{b}_2 \approx \bar{b}_3 = \bar{b}$ for some reasonable value of \bar{b} , and thereby obtain a further constraint on A_5 and C_5 . One would then have, instead of (69) and (70),

$$G^{(0)} \approx \frac{2}{\kappa_p} \left\{ G^{(1)} \left[C_5 + \frac{\alpha \kappa_p}{2} (\beta_1 + \beta_2 + \bar{b}) \right] + \bar{G}^{(1)} A_5 \right\}. \quad (72)$$

If the overall fit is not feasible, we would then be forced to work with the mean coefficient $\bar{G}^{(1)}$ as discussed in Sec. IIIA.

(vi) The measurement of the correlation parameter A_{LL} provides direct information on $\text{Re}(\Phi_1 - \Phi_3^N)$. We have

$$A_{LL} \frac{d\sigma}{dt} = I(L, L; 0, 0) = \frac{2\pi}{s(s-4m^2)} (|\Phi_1|^2 + |\Phi_2|^2 - |\Phi_3|^2 - |\Phi_4|^2) = 4\pi \left[\frac{\alpha}{t} (H^{(1)} - \alpha \bar{H}^{(1)} \ln|t|) + H^{(0)} \right], \quad (73)$$

with

$$H^{(1)} = C_1 - C_3, \quad (74)$$

$$\bar{H}^{(1)} = A_1 - A_3 = \frac{1}{8\pi} \Delta\sigma_L, \quad (75)$$

$$H^{(0)} = \frac{1}{4\pi} \left(A_{LL} \frac{d\sigma}{dt} \right)_{t=0}^N + \alpha \left[2\beta_1 (C_1 - C_3) + C_1 \bar{b}_1 - C_3 \bar{b}_3 + \frac{\kappa_p^2}{4m^2} C_2 \right], \quad (76)$$

in which

$$\frac{1}{4\pi} \left(A_{LL} \frac{d\sigma}{dt} \right)_{t=0}^N = \frac{1}{2} \left\{ \frac{\sigma_T}{4\pi} [A_1 - A_3 + \rho(C_1 - C_3)] + C_2^2 + A_2^2 \right\}. \quad (77)$$

Assuming $H^{(0)}$ is known, the interference fit directly tells us about $\text{Re}(\Phi_1^N - \Phi_3^N)$ which could then be compared with the value obtained in subsection (v).

It is unlikely that the correction terms in (77) could be important. If we try to neglect them, then (76) and (77) can be simplified to

$$H^{(0)} = \frac{1}{2} \left\{ \frac{\sigma_T}{4\pi} [\bar{H}^{(1)} + \rho H^{(1)}] + C_2^2 + A_2^2 \right\}. \quad (78)$$

A fit only to the A_{LL} interference still has four parameters. If we assume that C_2 and A_2 are known from the other interference measurements and that $H^{(0)}$ is known, then (51) could be used as a constraint on $H^{(1)}$ and $\bar{H}^{(1)}$ in the search.

(vii) The linear combination of target depolarization parameters $D_{LL} \sin \theta_R + D_{LS} \cos \theta_R$, where θ_R is the laboratory recoil angle, gives direct information on $\text{Re}\Phi_5^N$. We have¹⁶

$$\frac{d\sigma}{dt} D_{LL} \equiv I(0, L; 0, L), \quad (79)$$

$$\frac{d\sigma}{dt} D_{LS} \equiv I(0, L; 0, S), \quad (80)$$

and

$$(D_{LL} \sin \theta_R + D_{LS} \cos \theta_R) \frac{d\sigma}{dt} = \frac{-4\pi}{s(s-4m^2)} \text{Re}[\Phi_5^* (\Phi_1 - \Phi_2 + \Phi_3 - \Phi_4)]. \quad (81)$$

Then we find

$$\frac{m}{(-t)^{1/2}} (D_{LL} \sin \theta_R + D_{LS} \cos \theta_R) \frac{d\sigma}{dt} = 4\pi \left[-\frac{\alpha^2 \kappa_p}{2t^2} + \frac{\alpha}{t} (K^{(1)} - \alpha \bar{K}^{(1)} \ln|t|) + K^{(0)} \right], \quad (82)$$

where

$$K^{(1)} = -2C_5 + \frac{\kappa_p}{2} C_2 - \frac{\kappa_p}{8\pi} \rho \sigma_{\text{tot}}, \quad (83)$$

$$\begin{aligned} \bar{K}^{(1)} &= -\frac{\kappa_p}{2} (A_1 - A_2 + A_3) - 2A_5 \\ &= -\frac{\kappa_p}{8\pi} \sigma_{\text{tot}} + \frac{\kappa_p}{2} A_2 - 2A_5, \end{aligned} \quad (84)$$

and

$$\begin{aligned} K^{(0)} &= \frac{1}{4\pi} \left[\frac{m}{(-t)^{1/2}} (D_{LL} \sin \theta_R + D_{LS} \cos \theta_R) \frac{d\sigma}{dt} \right]_{t=0}^N \\ &\quad - \alpha \left[\left(-\frac{\kappa_p}{2} C_2 + \frac{\kappa_p}{8\pi} \rho \sigma_{\text{tot}} \right) (\beta_1 + \beta_2) \right. \\ &\quad \left. + \frac{\kappa_p}{2} \left(C_1 \bar{b}_1 - C_2 \bar{b}_2 + C_3 \bar{b}_3 - \frac{C_4}{m^2} \right) \right. \\ &\quad \left. + 2C_5 \left(2\beta_1 + \bar{b}_5 + \frac{\kappa_p^2}{4m^2} \right) \right], \end{aligned} \quad (85)$$

where

$$\begin{aligned} \frac{1}{4\pi} \left[\frac{m}{(-t)^{1/2}} (D_{LL} \sin \theta_R + D_{LS} \cos \theta_R) \frac{d\sigma}{dt} \right]_{t=0}^N \\ &= C_5 (C_1 - C_2 + C_3) + A_5 (A_1 - A_2 + A_3) \\ &= \frac{\sigma_{\text{tot}}}{4\pi} (A_5 + \rho C_5) - (C_5 C_2 + A_5 A_2). \end{aligned} \quad (86)$$

If $K^{(0)}$ is known, then an interference-region fit yields further constraints on the real and imaginary parts of Φ_5^N and Φ_2^N . The extraction of the nuclear part of $K^{(0)}$ is straightforward since the $O(\alpha)$ corrections in Eq. (85) are negligible.

(viii) In the above, we have focused upon the measurement of individual observables and we have discussed these measurements more or less in isolation. It is of interest to survey the overall picture assuming that all the above measurements have been carried out.

The interference measurement on

$$d\sigma/dt, Pd\sigma/dt, A_{NN}d\sigma/dt, A_{SS}d\sigma/dt,$$

$A_{LL}d\sigma/dt, D_{LL} \sin \theta_R + D_{LS} \cos \theta_R,$ and $A_{SL}d\sigma/dt$ yield, in principle, nineteen coefficients which are expressed in terms of seventeen hadronic parameters; the ten $t=0$ values A_i, C_i ($i=1;5$) and the slopes $b_1, b_2, b_3, b_5, \bar{b}_1, \bar{b}_2,$ and \bar{b}_3 . In addition there is also the constraint from σ_{tot} . Thus, in principle at least, the parameters are constrained and can be determined from a consistent set of experiments.

The principal results are summarized in Table I.

D. The general structure for $np \rightarrow np$ and $\Lambda p \rightarrow \Lambda p$

We shall discuss the general case $A+B \rightarrow A+B$, where A and B are nonidentical fermions. The

results for a particular reaction can then be read off quite simply. However, care must be taken in specifying the experimental observables since they are no longer symmetric between A and B .

We shall adopt the new "experimental" notation for the observables, $I(\hat{a}, \hat{b}; \hat{c}, \hat{d})$, in which the unit direction vectors are given in the order (beam, target; scattered, recoil) and in which each unit vector can lie along three possible directions: N for "normal" to the reaction plane, L for "longitudinal," i.e., along the particle's motion, and S for $N \times L$. The directions $N, L,$ and S are specified differently for each particle as can be seen in Fig. 9, and all refer to directions in the laboratory reference frame, i.e., the target rest frame. The normalization is defined so that $I(0, 0; 0, 0) = d\sigma/dt$.

The formulas we list apply to the case where the beam and scattered particles, i.e., particles $A,$ are uncharged. Examples are the reactions $np \rightarrow np$ or $\Lambda p \rightarrow \Lambda p$.

Because particle A has a zero charge, we have

$$F_1^A(q^2=0) = 0, \quad (87)$$

and thus the infinite phase term $i\alpha F_1^A F_1^B \ln \lambda^2$ and the enhanced terms $i\alpha F_1^A F_1^B \ln |t|$ no longer appear. The structure of the interference is therefore much simpler than in the proton-proton case. On the other hand, the interference is harder to detect because of the absence of α^2/t^2 terms.

The most general structure we shall encounter for an observable X is now [compare with (28)]

$$X(t) = \frac{\alpha}{(-t)^{1/2}} X^{(1)} + (-t)^{1/2} X^{(0)}. \quad (88)$$

The coefficients $X^{(1)}$ and $X^{(0)}$ are mixtures of hadronic and electromagnetic quantities.

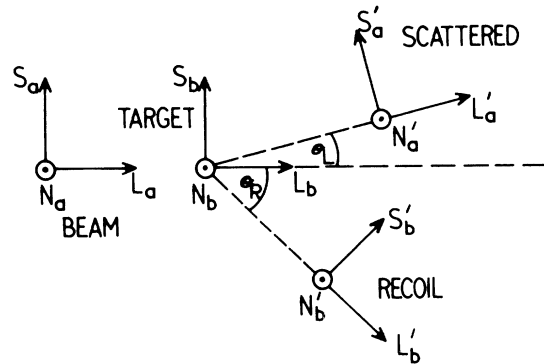


FIG. 9. Definition of the polarization directions N, L, S for the various particles in the reaction $A+B \rightarrow A'+B'$, all in the laboratory frame.

An immediate and important distinction between the present case and proton-proton scattering is the specification of the interference region. In the present case this is not always the region $|t| \lesssim \alpha$ (GeV/c)²; but sometimes, depending on the observables, is $(-t)^{1/2} \lesssim \alpha$ (GeV/c), i.e., $|t| \lesssim 10^{-4}$ (GeV/c)². The measurements of such tiny recoil energies is a great challenge but appears to be feasible with the development of gas-jet targets.

A second, and perhaps surprising difference, is that the measurement of ρ , the ratio of real to imaginary parts of the nonflip amplitudes, is exceedingly difficult, whereas in $pp - pp$ it is the simplest of all phases to determine.

We turn now to the detailed formulas.

E. Interference measurements for $A + B \rightarrow A + B$

We stress again that the interference measurements give direct information about the "contaminated nuclear amplitudes" parametrized as in Eqs. (19), (26), and (40).

(i) The invariant differential cross section gives no information about the hadronic amplitudes from interference. But it does diverge as $t \rightarrow 0$, though only as $1/t$ with a known coefficient.

We have

$$\begin{aligned} \frac{d\sigma}{dt} &= \frac{2\pi}{(s - \Delta^2)(s - \Sigma^2)} (|\Phi_1|^2 + |\Phi_2|^2 + |\Phi_3|^2 \\ &\quad + |\Phi_4|^2 + 2|\Phi_5|^2 + 2|\Phi_6|^2) \\ &= 4\pi \left(-\frac{\alpha^2 \kappa_A^2}{4m_A^2} \frac{1}{t} + I^{(0)} \right), \end{aligned} \quad (89)$$

where

$$\begin{aligned} I^{(0)} &= \frac{1}{4\pi} \left(\frac{d\sigma}{dt} \right)_{t=0}^N \\ &\quad + \alpha \left[-\tilde{F}_1^A (C_1 + C_3) + \frac{\kappa_A \kappa_B}{4m_A m_B} C_2 + \frac{\kappa_A}{m_A^2} C_5 \right]. \end{aligned} \quad (90)$$

We recall that Δ and Σ were defined in Sec. II E.

The region of interference is $|t| \sim \alpha^2$ (GeV/c)², and we should be able to detect the sharp rise in the measured $d\sigma/dt$ in this region. The detection of the rise does not provide any hadronic information, but would be a beautiful phenomenon to observe as a general test of the technical feasibility of probing such small values of momentum transfer.

The $O(\alpha)$ connections in (90) are quite negligible so that the measurement of $I^{(0)}$ provides information on

$$\begin{aligned} \frac{1}{4\pi} \left(\frac{d\sigma}{dt} \right)_{t=0}^N &= \left(\frac{\sigma_T}{8\pi} \right)^2 (1 + \rho^2) + \frac{1}{4} (C_1 - C_3)^2 + \frac{1}{4} (A_1 - A_3)^2 \\ &\quad + \frac{1}{2} (C_2^2 + A_2^2). \end{aligned} \quad (91)$$

The difficulties of normalization involved in the use of neutral beams make it unlikely that a precise value of ρ could be obtained from Eq. (91).

(ii) The polarization P_A of the fast forward-scattered particle A for an unpolarized beam and target has the most dramatic behavior of all the observables. This remarkable phenomenon was discovered by Schwinger as early as 1948 and was suggested by him as a method for producing an almost 100% polarized beam of neutrons.

We find

$$\begin{aligned} P_A \frac{d\sigma}{dt} &= \frac{4\pi}{(s - \Delta^2)(s - \Sigma^2)} \\ &\quad \times \text{Im}[\Phi_6^*(\Phi_1 + \Phi_3) - \Phi_5^*(\Phi_2 - \Phi_4)] \end{aligned} \quad (92)$$

and

$$\frac{m_A}{(-t)^{1/2}} P_A \frac{d\sigma}{dt} = 4\pi \left(-\frac{\alpha}{t} B_A^{(1)} + B_A^{(0)} \right), \quad (93)$$

where

$$B_A^{(1)} = \kappa_A \frac{\sigma_{\text{tot}}}{8\pi} \quad (94)$$

and

$$\begin{aligned} B_A^{(0)} &= \left(\frac{m_A}{4\pi(-t)^{1/2}} P_A \frac{d\sigma}{dt} \right)_{t=0}^N \\ &\quad - \alpha \left[\kappa_A \frac{\sigma_{\text{tot}}}{8\pi} (\beta_1^B + \beta_2^A) + \frac{\kappa_A}{2} (A_1 b_1 + A_3 b_3) \right. \\ &\quad \left. - \tilde{F}_1^A \left(2A_6 + \frac{m_A \kappa_B}{2m_B} A_2 \right) - \frac{\kappa_A \kappa_B}{2m_B^2} A_5 \right], \end{aligned} \quad (95)$$

in which

$$\begin{aligned} \left(\frac{m_A}{4\pi(-t)^{1/2}} P_A \frac{d\sigma}{dt} \right)_{t=0}^N &= \frac{\sigma_{\text{tot}}}{4\pi} (C_6 - \rho A_6) \\ &\quad - \frac{m_A}{m_B} (A_2 C_5 - A_5 C_2). \end{aligned} \quad (96)$$

First, we shall consider the region of *very* small t , i.e., $|t| \sim \alpha^2$ (GeV/c)² and suppose that there is zero *hadronic* polarization, namely zero hadronic helicity flip, so that only the $B_A^{(1)}$ term need be kept in Eq. (93). Using (89) for $d\sigma/dt$ we see that

$$P_A = \frac{\alpha \kappa_A}{m_A} \frac{\sigma_{\text{tot}}}{8\pi} \frac{(-t)^{1/2}}{\alpha^2 \kappa_A^2 / 4m_A^2 - t I^{(0)}} \quad (97)$$

has a maximum at

$$t = t_M = -\frac{\alpha^2 \kappa_A^2}{4m_A^2} \frac{1}{I^{(0)}}, \quad (98)$$

which is also the point of maximum interference in $d\sigma/dt$. At this point

$$P_A = P^{\max} = \frac{\sigma_{\text{tot}}}{8\pi(I^{(0)})^{1/2}} \approx \frac{\sigma_{\text{tot}}}{8\pi([(1/4\pi)d\sigma/dt]_{t=0}^N)^{1/2}}. \quad (99)$$

Thus, the Schwinger polarization is gigantic. If we approximate the nuclear differential cross section by its optical value $\sigma_{\text{tot}}^2/16\pi$, we arrive at

$$P_A^{\max} = 1,$$

i.e., 100% polarization at $t = t_M \approx -0.6 \times 10^{-5}$ (GeV/c)².

The correction terms to t_M and P_A^{\max} arising from the $B_A^{(0)}$ term in (93) are quite negligible. On the other hand, hadronic real part effects, nonzero values of the amplitudes $\Phi_2^N(t=0)$, and the possible nonequality of Φ_1^N and Φ_3^N at $t=0$ will reduce P_A^{\max} to below the 100% optical value, and might even serve as a rough measure of ρ .

Considering that the electromagnetically induced polarization is so much larger in $np \rightarrow np$ than it is in $pp \rightarrow pp$, it is all the more necessary to exercise care when interpreting measurements of the polarization *outside* the interference region if the measured polarizations are small. We have repeated, for the case of $np \rightarrow np$, the calculation described in Sec. III C (ii), and the resulting polarization P_n is shown in Fig. 10.

In order to extricate the nuclear polarization from the measured value of $B_A^{(0)}$ outside the interference region, it is probably adequate to approximate (95) by [see (57) and discussion preceding it]

$$B_A^{(0)} = \left(\frac{m_A}{4\pi(-t)^{1/2}} P_A \frac{d\sigma}{dt} \right)_{t=0}^N - \frac{\alpha \sigma_{\text{tot}}}{8\pi} \kappa_A (\beta_1^B + \beta_2^A + b), \quad (100)$$

where $2b$ is the logarithmic slope of $(d\sigma/dt)^N$ at $t=0$.

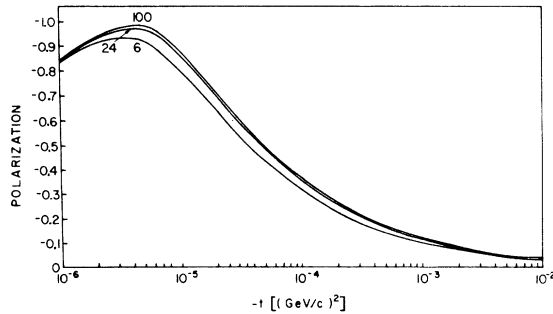


FIG. 10. Electromagnetically induced polarization P_n of the neutron in the reaction $np \rightarrow np$ at several laboratory momenta.

(iii) The polarization P_B of particle B , which could be measured for $np \rightarrow np$ and $\Lambda p \rightarrow \Lambda p$ by use of a polarized proton target (it should strictly be called the "asymmetry" in this type of experiment), gives direct information on the imaginary part of Φ_2^N .

A comparison of Φ_2^N for $np \rightarrow np$ and $pp \rightarrow pp$ would be of great interest. We have

$$P_B \frac{d\sigma}{dt} = \frac{-4\pi}{(s-\Delta^2)(s-\Sigma^2)} \text{Im}[\Phi_5^*(\Phi_1 + \Phi_3) - \Phi_6^*(\Phi_2 - \Phi_4)], \quad (101)$$

and we find

$$\frac{m_A}{(-t)^{1/2}} P_B \frac{d\sigma}{dt} = 4\pi \left(-\frac{\alpha}{t} B_B^{(1)} + B_B^{(0)} \right), \quad (102)$$

where

$$B_B^{(1)} = \frac{\kappa_A A_2}{2} \quad (103)$$

and

$$B_B^{(0)} = \left(\frac{m_A}{4\pi(-t)^{1/2}} P_B \frac{d\sigma}{dt} \right)_{t=0}^N - \alpha \left\{ \bar{F}_1^A \left(2A_5 - \frac{\kappa_B \sigma_{\text{tot}}}{8\pi} \right) + \frac{\kappa_A}{2} \left[A_2(\beta_1^B + \beta_2^A + b_2) + \frac{A_4}{m_A m_B} \right] + \frac{\kappa_A \kappa_B}{2 m_A m_B} A_6 \right\}, \quad (104)$$

in which

$$\begin{aligned} \frac{m_A}{4\pi} \left(\frac{1}{(-t)^{1/2}} P_B \frac{d\sigma}{dt} \right)_{t=0}^N &= -\frac{m_A}{m_B} [C_5(A_1 + A_3) - A_5(C_1 + C_3)] + C_6 A_2 - A_6 C_2 \\ &= -\frac{m_A}{m_B} \frac{\sigma_{\text{tot}}}{4\pi} (C_5 - \rho A_5) + C_6 A_2 - A_6 C_2. \end{aligned} \quad (105)$$

As usual, caution is necessary in extracting the nuclear part of the polarization from a knowledge of $B_B^{(0)}$ and (104). An adequate approximation to (104) would be provided by taking

$$B_B^{(0)} \approx \left(\frac{m_A}{4\pi(-t)^{1/2}} P_B \frac{d\sigma}{dt} \right)_{t=0}^N + \frac{\alpha \bar{F}_1^A \kappa_B \sigma_{\text{tot}}}{8\pi}. \quad (106)$$

(iv) Neither $A_{NN}d\sigma/dt$ nor $A_{SS}d\sigma/dt$ show any interference effects. However, $A_{SL}d\sigma/dt$ provides us with a direct measurement of the real part of $\Phi_1^N - \Phi_3^N$. We have

$$A_{SL} \frac{d\sigma}{dt} = I(S, L; 0, 0) \\ = \frac{-4\pi}{(s - \Delta^2)(s - \Sigma^2)} \\ \times \text{Re}[\Phi_6^*(\Phi_1 - \Phi_3) - \Phi_5^*(\Phi_2 + \Phi_4)], \quad (107)$$

and find

$$\frac{m_A}{(-t)^{1/2}} A_{SL} \frac{d\sigma}{dt} = 4\pi \left[\frac{\alpha}{t} G_A^{(1)} + G_A^{(0)} \right], \quad (108)$$

where

$$G_A^{(1)} = \frac{\kappa_A}{2} (C_1 - C_3) \quad (109)$$

and

$$G_A^{(0)} = \left(\frac{1}{4\pi} \frac{m_A}{(-t)^{1/2}} A_{SL} \frac{d\sigma}{dt} \right)_{t=0}^N \\ + \alpha \left\{ \frac{\kappa_A}{2} [C_1(\beta_1^B + \beta_2^A + \bar{b}_1) - C_3(\beta_1^B + \beta_2^A + \bar{b}_3)] - \frac{\kappa_B m_A \bar{F}_1^A}{2m_B} C_2 \right\}, \quad (110)$$

in which

$$\left(\frac{1}{4\pi} \frac{m_A}{(-t)^{1/2}} A_{SL} \frac{d\sigma}{dt} \right)_{t=0}^N = (C_3 - C_1)C_6 + (A_3 - A_1)A_6 \\ + \frac{m_A}{m_B} (C_2C_5 + A_5A_2). \quad (111)$$

Assuming $G_A^{(0)}$ is known, the interference measurement should provide a reliable value of $G_A^{(1)}$ and thus of the real part difference $C_1 - C_3$. The $O(\alpha)$ correction terms in (110) are almost certainly negligible when extracting the nuclear $(A_{SL} d\sigma/dt)_{t=0}^N$ from the value of $G_A^{(0)}$.

(v) Because the particles A and B are nonidentical, we have $A_{LS} \neq A_{SL}$ and, indeed, A_{LS} gives us new information on the real part of Φ_2^N . This complements the measurement of $\text{Im}\Phi_2^N$ in subsection (iii) above.

We have

$$A_{LS} \frac{d\sigma}{dt} = I(L, S; 0, 0) \\ = \frac{4\pi}{(s - \Delta^2)(s - \Sigma^2)} \\ \times \text{Re}[\Phi_5^*(\Phi_1 - \Phi_3) - \Phi_6^*(\Phi_2 + \Phi_4)], \quad (112)$$

and find

$$\frac{m_A}{(-t)^{1/2}} A_{LS} \frac{d\sigma}{dt} = 4\pi \left(\frac{\alpha}{t} G_B^{(1)} + G_B^{(0)} \right) \quad (113)$$

with

$$G_B^{(1)} = \frac{\kappa_A}{2} C_2 \quad (114)$$

and

$$G_B^{(0)} = \left(\frac{1}{4\pi} \frac{m_A}{(-t)^{1/2}} A_{LS} \frac{d\sigma}{dt} \right)_{t=0}^N \\ + \alpha \left\{ \frac{\kappa_A}{2} \left[C_2(\beta_1^B + \beta_2^A + \bar{b}_2) - \frac{C_4}{m_A m_B} \right] - \bar{F}_1^A \frac{\kappa_B m_A}{2m_B} (C_1 - C_3) \right\}, \quad (115)$$

in which

$$\left(\frac{1}{4\pi} \frac{m_A}{(-t)^{1/2}} A_{LS} \frac{d\sigma}{dt} \right)_{t=0}^N \\ = \frac{m_A}{m_B} [C_5(C_1 - C_3) + A_5(A_1 - A_3)] \\ - (C_6C_2 + A_6A_2). \quad (116)$$

The $O(\alpha)$ correction terms in (115) are almost certainly negligible.

(vi) The correlation parameter A_{LL} does not show interference effects. However, its value at small t is interesting, being a direct measure of $|\Phi_1^N|^2 - |\Phi_3^N|^2$.

(vii) In total we see that feasible interference measurements on $A+B \rightarrow A+B$, A neutral, B charged, yield information about the "contaminated" nuclear amplitudes Φ_2^N (real and imaginary parts) and $\text{Re}(\Phi_1^N - \Phi_3^N)$. The measurement of P_A at maximum would help to evaluate $\text{Re}(\Phi_1^N + \Phi_3^N)$, which is otherwise difficult to measure, but this would not be an accurate determination.

It appears that the most direct way to measure ρ , at least for $np \rightarrow np$, is to study the depolarization parameters of the neutron. As we shall see, this can be done in two ways, neither of which is simple experimentally.

It has to be remembered that in a reaction $AB \rightarrow AB$ we can define two independent depolarization parameters $D_{ij}^{(A)}$ and $D_{ij}^{(B)}$. Moreover, the labels (i, j) , say, for particle A have a quite different meaning in the reaction $AB \rightarrow AB$, where A is the beam particle, and in the reaction $BA \rightarrow BA$, where A is the target particle.

In the "experimental notation¹⁵" we consider the following parameters for A :

$$\frac{d\sigma}{dt} D_{LS}^{(A)}(AB \rightarrow AB) \equiv I(L, 0; L, 0)_{AB \rightarrow AB},$$

$$\frac{d\sigma}{dt} D_{LL}^{(A)}(AB \rightarrow AB) \equiv I(L, 0; S, 0)_{AB \rightarrow AB},$$

relevant to experiments in which particle A is the beam particle, and

$$\frac{d\sigma}{dt} D_{LL}^{(A)}(BA \rightarrow BA) \equiv I(0, L; 0, L)_{BA \rightarrow BA},$$

$$\frac{d\sigma}{dt} D_{LS}^{(A)}(BA \rightarrow BA) \equiv I(0, L; 0, S)_{BA \rightarrow BA},$$

relevant when particle A is the target particle.

In the case of the neutron-proton reaction one could use a polarized neutron beam and then have the difficulty of analyzing the polarization of the fast-scattered neutron, or one could use a polarized deuterium target and then face the difficulty of analyzing the polarization of the recoil neutron. For Λ -proton reactions, however, it might be feasible to measure $D^{(A)}$ using a polarized Λ beam on an unpolarized proton target.

In either experimental approach, the useful combination of experimental quantities is

$$\begin{aligned} \mathfrak{D} &\equiv \left((D_{LL}^{(A)} \sin \theta_R + D_{LS}^{(A)} \cos \theta_R) \frac{d\sigma}{dt} \right)_{BA \rightarrow BA} \\ &= \left((D_{LL}^{(A)} \sin \theta_L - D_{LS}^{(A)} \cos \theta_L) \frac{d\sigma}{dt} \right)_{AB \rightarrow AB} \\ &= \frac{4\pi}{(s - \Delta^2)(s - \Sigma^2)} \operatorname{Re}[\Phi_6^*(\Phi_1 + \Phi_3) + \Phi_5^*(\Phi_2 - \Phi_4)], \end{aligned} \quad (117)$$

in which, as always, the actual helicity amplitudes refer to the process $AB \rightarrow AB$. As usual, θ_L and θ_R refer to the laboratory scattering and recoil angles, respectively.

One finds

$$\frac{m_A}{(-t)^{1/2}} \mathfrak{D} = 4\pi \left(-\frac{\alpha}{t} L^{(1)} + L^{(0)} \right), \quad (118)$$

where

$$L^{(1)} = \frac{\kappa_A}{2} (C_1 + C_3) \quad (119)$$

and

$$\begin{aligned} L^{(0)} &= \left(\frac{1}{4\pi} \frac{m_A}{(-t)^{1/2}} \mathfrak{D} \right)_{t=0}^N \\ &\alpha \left\{ \frac{\kappa_A}{2} \left[C_1(\beta_1^B + \beta_2^A + \bar{b}_1) \right. \right. \\ &\quad \left. \left. + C_3(\beta_1^B + \beta_2^A + \bar{b}_3) - \frac{\kappa_B}{m_A m_B} C_5 \right] \right. \\ &\quad \left. + \bar{F}_1^A \left(C_6 + \frac{\kappa_B}{2} \frac{m_A}{m_B} C_2 \right) \right\}, \end{aligned} \quad (120)$$

in which

$$\begin{aligned} \left(\frac{1}{4\pi} \frac{m_A}{(-t)^{1/2}} \mathfrak{D} \right)_{t=0}^N &= C_6(C_1 + C_3) + A_6(A_1 + A_3) \\ &\quad + \frac{m_A}{m_B} (C_5 C_2 + A_5 A_2). \end{aligned} \quad (121)$$

Thus the coefficient of α/t directly measures $C_1 + C_3$. It is remarkable that the determination of $\operatorname{Re}(\Phi_1^N + \Phi_3^N)$ for the collision of neutral and charged particles should prove such a difficult task experimentally.

The main results are summarized in Table I.

IV. EXTRACTION OF THE "PURE" NUCLEAR AMPLITUDES

In the previous section we saw how measurements made in the interference region can provide us with information about the "contaminated nuclear amplitude" Φ_i^N which corresponds to the sum of diagrams shown in Fig. 6. The difference between the Φ_i^N and the "pure nuclear amplitude" ϕ_i^N is of the order α in general, but, due to the spin structure and the fact that some helicity amplitudes are much smaller than others, it can be relatively enhanced in certain cases. For the sake of completeness, we discuss the derivation of the exact results in Appendix C. Here we shall only be concerned with the dominant, "enhanced $O(\alpha)$ " corrections to the measured combinations of Φ_i^N .

The logarithmic slopes, b_i, \bar{b}_i of the contaminated nuclear amplitude Φ_i^N differ only negligibly from those of the pure nuclear amplitudes. Therefore, we shall not distinguish between them in this section.

The method which we have used in calculating the Φ_i^N from the ϕ_i^N was explained in Sec. II, and is valid at high energies and moderate momentum transfers. The parametrization of the ϕ_i^N and ϕ_i^{EM} required in this calculation is given in Eqs. (19), (20), (26), and (34)–(39). Inaccuracies in this parametrization at large t will be reflected in growing uncertainty in the Φ_i^N for large t .

We treat the cases $pp \rightarrow pp$ and $AB \rightarrow AB$ separately.

A. Proton-proton scattering

Corrections to the sum of the imaginary parts of the nonflip amplitudes are negligible and, thus we find

$$A_1 + A_3 = a_1 + a_3. \quad (122)$$

If the real parts are small, then the corrections could be moderately important. We have

$$\begin{aligned} C_1 &\approx c_1 - \alpha a_1 [\gamma + \ln(2\beta_1 + b_1)], \\ C_3 &\approx c_3 - \alpha a_3 [\gamma + \ln(2\beta_1 + b_3)], \end{aligned} \quad (123)$$

where $\gamma = 0.5772$ is Euler's constant. Taking $b_1 \approx b_3 = b$, where $2b$ is roughly the logarithmic slope of $(d\sigma/dt)^N$, we have

$$c_1 + c_3 \approx C_1 + C_3 + \frac{\alpha \sigma_{\text{tot}}}{4\pi} [\gamma + \ln(2\beta_1 + b)]. \quad (124)$$

For the difference between Φ_1^N and Φ_3^N we have, to a good approximation,

$$A_1 - A_3 = a_1 - a_3 + \frac{\alpha\kappa^2}{4m^2} \frac{c_2}{\bar{b}_2 + 2\beta_2} + \frac{c_4}{m^2(\bar{b}_4 + 2\beta_2)^2},$$

$$C_1 - C_3 = c_1 - c_3 - \frac{\alpha\kappa^2}{4m^2} \frac{a_2}{\bar{b}_2 + 2\beta_2} + \frac{a_4}{m^2(\bar{b}_4 + 2\beta_2)^2}. \quad (125)$$

The correction terms are unenhanced so that only if the differences $A_1 - A_3$, $C_1 - C_3$ are exceedingly small is it necessary to use (125) to estimate $a_1 - a_3$ or $c_1 - c_3$.

One of the most interesting cases is the amplitude Φ_2^N . We have

$$A_2 \approx a_2 + \alpha \left\{ c_2 [\gamma + \ln(2\beta_1 + \bar{b}_2)] + \frac{\kappa_2}{4m^2} \frac{c_1}{b_1 + 2\beta_2} - \frac{\kappa c_5}{m^2(\beta_1 + \beta_2 + \bar{b}_5)} \right\} \quad (126)$$

and

$$C_2 \approx c_2 - \alpha \left\{ a_2 [\gamma + \ln(2\beta_1 + b_2)] + \frac{\kappa^2}{4m^2} \frac{a_1}{b_1 + 2\beta_2} - \frac{\kappa a_5}{m^2(\beta_1 + \beta_2 + b_5)} \right\}. \quad (127)$$

Let us estimate the correction to C_2 by keeping only the term involving a_1 in (127). If we take $a_1 \approx A_1 = \sigma_{\text{tot}}/8\pi$, $b_1 \approx b$, we have

$$C_2 \approx c_2 - \frac{\alpha\kappa^2}{4m^2} \frac{\sigma_{\text{tot}}}{8\pi} \frac{1}{b + 2\beta_2}. \quad (128)$$

It is instructive to compare the correction term to the usual pion contribution to C_2 . In $pp \rightarrow pp$,

$$\phi_2^N(\pi + \pi_{\text{cut}}) \approx \frac{1}{2} \frac{g^2}{4\pi} \frac{m_\pi^2}{(t - m_\pi^2)} e^{5.5t},$$

therefore,

$$c_2(\pi + \pi_{\text{cut}}) = -\frac{1}{2S} \frac{g^2}{4\pi},$$

whereas the correction term has the same sign as $c_2(\pi + \pi_{\text{cut}})$ and

$$\frac{\text{correction term}}{c_2(\pi + \pi_{\text{cut}})} \approx \frac{\alpha p_L}{b + 2\beta_2} \approx 30\%$$

at $p_L = 300 \text{ GeV}/c$. This correction is perhaps important in elastic pp scattering if measurements of C_{NN} become possible at Fermilab. At higher energies the correction could actually dominate.

In a similar approximation, the correction to C_4 is

$$C_4 \approx c_4 + \frac{\alpha\kappa^2\sigma_{\text{tot}}b^2}{64\pi(2\beta_2 + b)^2}, \quad (129)$$

which could be important at Fermilab energies. Corrections to A_4 are negligible.

For Φ_5 only the correction to C_5 might be important. The dominant term is approximately

$$C_5 \approx c_5 + \frac{\alpha\kappa\sigma_{\text{tot}}b}{16\pi(\beta_1 + \beta_2 + b)} \quad (130)$$

B. $A + B \rightarrow A + B$; A neutral

For the nonflip amplitudes we get

$$A_1 + A_3 \approx a_1 + a_3$$

and, keeping the dominant term only,

$$C_{1,3} \approx c_{1,3} + \frac{\alpha\bar{F}_1^A\sigma_{\text{tot}}}{8\pi(\beta_1^A + \beta_2^B + b)} \quad (131)$$

For the differences between Φ_1^N and Φ_3^N we have

$$A_1 - A_3 \approx a_1 - a_3 + \frac{\alpha\kappa_A\kappa_B}{4m_A m_B} \left(\frac{c_2}{\bar{b}_2 + \beta_2^B + \beta_2^A} + \frac{c_4}{m_A m_B (\bar{b}_4 + \beta_2^A + \beta_2^A)^2} \right) \quad (132)$$

and

$$C_1 - C_3 \approx c_1 - c_3 - \frac{\alpha\kappa_A\kappa_B}{4m_A m_B} \left(\frac{a_4}{b_2 + \beta_2^B + \beta_2^A} + \frac{a_2}{m_A m_B (b_4 + \beta_2^A + \beta_2^B)^2} \right) \quad (133)$$

so that the correction is negligible unless the differences are exceedingly small.

The corrections to $\text{Im } \Phi_2^N$ and $\text{Im } \Phi_4^N$ are negligible, but for $\text{Re } \Phi_2^N$ and $\text{Re } \Phi_4^N$ the dominant terms are analogous to the proton-proton case, i.e.,

$$C_2 \approx c_2 - \frac{\alpha\kappa_A\kappa_B}{4m_A m_B} \frac{\sigma_{\text{tot}}}{8\pi(b + \beta_2^B + \beta_2^A)} \quad (134)$$

and

$$C_4 \approx c_4 + \frac{\alpha\kappa_A\kappa_B\sigma_{\text{tot}}b^2}{64\pi(\beta_2^A + \beta_2^B + b)^2}. \quad (135)$$

Finally, for $\text{Re } \Phi_5^N$ we have

$$C_5 = c_5 + \frac{\alpha\kappa_B\bar{F}_1^A\sigma_{\text{tot}}b}{16\pi(b + \beta_1^A + \beta_2^B)^2} \quad (136)$$

and for $\text{Re } \Phi_6^N$

$$C_6 \approx c_6 - \frac{\alpha\kappa_A\sigma_{\text{tot}}b}{32\pi(b + \beta_1^B + \beta_2^A)} = -c_5 - \frac{\alpha\kappa_A\sigma_{\text{tot}}b}{32\pi(b + \beta_1^B + \beta_2^A)}. \quad (137)$$

Thus $C_5 \neq -C_6$ and similarly $A_5 \neq -A_6$, and the differences could be relatively significant if the amplitudes are *very* small.

V. CONCLUSIONS

The interference between electromagnetic and hadronic forces in the collision of spin- $\frac{1}{2}$ hadrons gives rise to remarkable spin-dependent phenomena at very small values of momentum transfer. These phenomena occur both in the collision of charged particles and in the collision between neutral and charged particles. The detection and measurement of such effects is technically difficult and presents a great challenge to the experimenter.

We have shown that the successful measurement of the interference effects will yield much information about the real and imaginary parts of the helicity-flip amplitudes near the forward direction. For the case of neutral-charged collisions one will, in addition, be able to measure the real part of the nonflip amplitude, a quantity that cannot be determined from classical Coulomb interference experiment.

We have also pointed out that electromagnetically induced spin-flip transitions can give rise, even in the absence of hadronic spin flip to nonsubstantial values of polarization parameters

and spin-correlation parameters well outside the interference region. This fact will strongly influence the interpretation of the small measured polarization values at Fermilab energies.

We have demonstrated that the Coulomb phase is insensitive to the spin of the particles involved and is therefore the same in all helicity amplitudes. On the other hand, we have found new "enhanced" order- α corrections resulting explicitly from the spin structure that could be important in determining the "pure" hadronic amplitudes from the experimentally measured ones.

Our treatment of the electromagnetic corrections appears to be a consistent one and the general techniques involved can also be used for calculating absorptive corrections in nucleon-nucleon scattering.

ACKNOWLEDGMENTS

E. G. is grateful to the Israel Commission for Basic Research and to the United Kingdom Science Research Council for financial support. E. L. also wishes to thank the U.K.S.R.C. for its generous support, and to acknowledge an award under the Royal Society-Israel Academy Programme. Our interest in this problem stems from discussions with Professor Martin Bloch.

APPENDIX A: ONE-PHOTON-EXCHANGE AMPLITUDES

Using the normalization convention described in Eq. (13), the exact one-photon-exchange contributions to the process $A + B \rightarrow A + B$, with allowances for form factors, are

$$\begin{aligned}
\alpha^{-1} \phi_1^{\text{em}}(s, t) &= F_1^A(q^2) F_1^B(q^2) \left(\frac{s - m_A^2 - m_B^2}{t} + \frac{m_A^2 + m_B^2 + (m_B^2 - m_A^2)^2/s}{4k^2} \right) \\
&\quad - \kappa_A F_2^A(q^2) F_1^B(q^2) - \kappa_B F_2^B(q^2) F_1^A(q^2) - \frac{\kappa_A \kappa_B}{2} F_2^A(q^2) F_2^B(q^2) \left(1 - \frac{t}{4k^2} \right), \\
\alpha^{-1} \phi_2^{\text{em}}(s, t) &= \frac{F_1^A(q^2) F_1^B(q^2) m_A m_B}{2k^2} - \frac{\kappa_A m_B}{2m_A} F_2^A(q^2) F_1^B(q^2) - \frac{\kappa_B m_A}{2m_B} F_2^B(q^2) F_1^A(q^2) \\
&\quad + \frac{\kappa_A \kappa_B}{4m_A m_B} F_2^A(q^2) F_2^B(q^2) \left[s - m_A^2 - m_B^2 + \frac{t}{8k^2} \left(s + \frac{(m_B^2 - m_A^2)^2}{s} \right) \right], \\
\alpha^{-1} \phi_3^{\text{em}}(s, t) &= \left[F_1^A(q^2) F_1^B(q^2) \frac{s - m_A^2 - m_B^2}{t} + \frac{\kappa_A \kappa_B F_2^A(q^2) F_2^B(q^2)}{2} \right] \left(1 + \frac{t}{4k^2} \right), \\
\phi_4^{\text{em}}(s, t) &= -\phi_2^{\text{em}}(s, t), \\
\alpha^{-1} \phi_5^{\text{em}}(s, t) &= \left[\frac{s}{-t} (4k^2 + t) \right]^{1/2} \left[\frac{F_1^A(q^2) F_1^B(q^2) m_A}{4k^2} \left(1 + \frac{m_A^2 - m_B^2}{s} \right) - \frac{\kappa_B}{2m_B} F_1^A(q^2) F_2^B(q^2) \right. \\
&\quad \left. + \frac{\kappa_A \kappa_B F_2^A(q^2) F_2^B(q^2)}{4m_B} \frac{t}{4k^2} \left(1 + \frac{m_B^2 - m_A^2}{s} \right) \right], \\
\alpha^{-1} \phi_6^{\text{em}}(s, t) &= \left[\frac{s}{-t} (4k^2 + t) \right]^{1/2} \left[\frac{-F_1^A(q^2) F_1^B(q^2) m_B}{4k^2} \left(1 + \frac{m_B^2 - m_A^2}{s} \right) + \frac{\kappa_A}{2m_A} F_2^A(q^2) F_1^B(q^2) \right. \\
&\quad \left. - \frac{\kappa_A \kappa_B F_2^A(q^2) F_2^B(q^2)}{4m_A} \frac{t}{4k^2} \left(1 + \frac{m_A^2 - m_B^2}{s} \right) \right],
\end{aligned} \tag{A1}$$

where $q^2 = -t$, and k is the c.m. momentum, so that

$$4k^2s = [s - (m_A + m_B)^2][s - (m_A - m_B)^2]. \quad (\text{A2})$$

In the case that A and B are the same particle we find, as expected, that

$$\phi_6 = -\phi_5. \quad (\text{A3})$$

The leading terms at high energy are displayed in Eqs. (34)–(36). For the calculation of the diagrams in Fig. 6 we use only the high-energy approximation, but for the numerical estimate of the polarization and C_{NN} in Sec. III C, we have used the exact results.

We note that the crossed one-photon diagram, corresponding to the exchange of a photon in the u channel, gives contributions that are totally negligible in the small- t region at high energies, as a consequence of the rapid falloff of the form factors.

APPENDIX B: THE b -SPACE TRANSFORMS

The fixed-impact-parameter amplitudes $\hat{\phi}_i(s, b)$ are described in Sec. II. Here we write down the relations between a given $\phi_i(s, t)$ and its transform $\hat{\phi}_i(s, b)$.

The Jacob-Wick partial-wave expansion is modified as follows:

(i) For $M \equiv \max\{\lambda, \mu\} \geq 0$,

$$d_{\lambda\mu}^J(\theta) \rightarrow (-1)^{N-\mu} J_{|\lambda-\mu|}(bq), \quad (\text{B1})$$

where $N = \min\{\lambda, \mu\}$, $b = (J + \frac{1}{2})/k$, and $q = (-t)^{1/2}$;

(ii) $\sum_J \rightarrow \int dJ = k \int db$;

(iii) $\langle \lambda' \mu' | T^J | \lambda \mu \rangle \rightarrow \hat{\phi}_{\lambda' \mu'; \lambda \mu}(s, b)$.

Bearing in mind our normalization, we have, at high energies, for $i = 1, \dots, 5$

$$\hat{\phi}_i(s, b) = \frac{2}{s} \int J_{|\lambda-\mu|}(bq) \phi_i(s, t) q dq, \quad (\text{B2})$$

$$\phi_i(s, t) = \frac{s}{2} \int J_{|\lambda-\mu|}(bq) \hat{\phi}_i(s, b) b db,$$

whereas, for $i = 6$,

$$\hat{\phi}_6(s, b) = -\frac{2}{s} \int J_1(bq) \phi_6(s, t) q dq,$$

$$\phi_6(s, t) = -\frac{s}{2} \int J_1(bq) \hat{\phi}_6(s, b) b db. \quad (\text{B3})$$

We note that if $A = B$ we will have

$$\hat{\phi}_6(s, b) = \hat{\phi}_5(s, b) \quad (\text{B4})$$

in contrast to Eq. (A 3).

The one-photon amplitudes

The $\phi_i^{\text{em}}(s, t)$ are parametrized as in Eqs. (34)–(36), and the form factors are parametrized as in Eqs. (38). We shall assume that neither $F_1^A(q^2)$ nor $F_1^B(q^2) = 0$ at $q^2 = 0$, i.e., we shall in fact pretend that both A and B are charged.

Since, for example, we parametrize

$$F_1^A(q^2) = F_1^A \exp(-\beta_1^A q^2) \quad (\text{B5})$$

when $F_1^A \neq 0$, and we use Eqs. (37) and (39)

$$F_1^A(q^2) = q^2 \tilde{F}_1^A \exp(-\beta_1^A q^2) \quad (\text{B6})$$

when $F_1^A(q^2 = 0) = 0$, it is clear that we can deduce results relevant to (B6), i.e., when say A is a neutral particle from those using (B5) by

(i) taking the derivative $-\partial/\partial\beta_1^A$ (B7)

(ii) replacing $F_1^A \rightarrow \tilde{F}_1^A$

Because of the masslessness of the photon, some of the b -space transforms diverge. It is thus necessary to give the photon a mass λ which is allowed to go to zero at the end of the calculation.

A very useful trick³ is to use the identity

$$\frac{1}{q^2 + \lambda^2} = \int_0^\infty e^{-x(q^2 + \lambda^2)} dx, \quad (\text{B8})$$

which then allows a simple evaluation of the b -space transforms.

In order to express the results succinctly, we define the following integral operator $I_x(\beta)$. For any reasonably behaved function $f(x)$, and for $\beta > 0$,

$$I_x(\beta) \{f(x)\} \equiv \int_\beta^\infty \frac{dx}{x} e^{-\lambda^2(x-\beta)} f(x). \quad (\text{B9})$$

We then find, using (B2) and (B3)

$$\begin{aligned} \hat{\phi}_1^{\text{em}}(s, b) &= \hat{\phi}_3^{\text{EM}}(s, b) = -\alpha F_1^A F_1^B I_x(\beta_1^A + \beta_2^B) \left\{ e^{-b^2/4x} \right\} \\ \hat{\phi}_2^{\text{EM}}(s, b) &= \frac{\alpha \kappa_A \kappa_B F_2^A F_2^B}{4m_A m_B} \exp \left[\frac{-b^2/4(\beta_2^A + \beta_2^B)}{\beta_2^A + \beta_2^B} \right], \\ \hat{\phi}_4^{\text{EM}}(s, b) &= \frac{-\alpha \kappa_A \kappa_B F_2^A F_2^B}{16m_A m_B} b^2 I_x(\beta_2^A + \beta_2^B) \left\{ \frac{e^{-b^2/4x}}{x^2} \right\} \\ \hat{\phi}_5^{\text{EM}}(s, b) &= \frac{-\alpha \kappa_B F_1^A F_2^B}{4m_B} b I_x(\beta_1^A + \beta_2^B) \left\{ \frac{e^{-b^2/4x}}{x} \right\} \\ \hat{\phi}_6^{\text{EM}}(s, b) &= \frac{-\alpha \kappa_A F_2^A F_1^B}{4m_A} b I_x(\beta_1^B + \beta_2^A) \left\{ \frac{e^{-b^2/4x}}{x} \right\} \end{aligned} \quad (\text{B10})$$

The "pure" nuclear amplitudes

Using the parametrization (20), as modified in (26), and taking

$$\begin{aligned} c_i(s, t) &= c_i \exp(\bar{b}_i t), \\ a_i(s, t) &= a_i \exp(b_i t), \end{aligned} \quad (\text{B11})$$

which is reasonable for a moderate range of t , we find for the b -space transforms of the $\phi_i^N(s, t)$,

$$\begin{aligned} \text{Re } \hat{\phi}_1^N(s, b) &= \frac{c_1}{b_1} \exp(-b^2/4\bar{b}_1), \\ \text{Re } \hat{\phi}_2^N(s, b) &= \frac{c_2}{b_2} \exp(-b^2/4\bar{b}_2), \\ \text{Re } \hat{\phi}_3^N(s, b) &= \frac{c_3}{b_3} \exp(-b^2/4\bar{b}_3), \\ \text{Re } \hat{\phi}_4^N(s, b) &= \frac{c_4}{4m_A m_B} \frac{b^2}{(\bar{b}_4)^2} \exp(-b^2/4\bar{b}_4), \\ \text{Re } \hat{\phi}_5^N(s, b) &= \frac{c_5}{2m_B} \frac{b}{(\bar{b}_5)^2} \exp(-b^2/4\bar{b}_5), \\ \text{Re } \hat{\phi}_6^N(s, b) &= \frac{-c_6}{2m_A} \frac{b}{(\bar{b}_6)^2} \exp(-b^2/4\bar{b}_6). \end{aligned} \quad (\text{B12})$$

Analogous expressions hold for the $\text{Im } \phi_i^N(s, b)$ which can be read off from (B12) with the replacements

$$\begin{aligned} c_i &\rightarrow a_i, \\ \bar{b}_i &\rightarrow b_i. \end{aligned} \quad (\text{B13})$$

Note that if particles A and B are identical, we would have $c_6 = -c_5$ and $\bar{b}_5 = \bar{b}_6$.

APPENDIX C: CALCULATION OF THE ‘‘CONTAMINATED’’ NUCLEAR AMPLITUDES

The ‘‘contaminated’’ nuclear amplitudes are defined diagrammatically in Fig. 6. We write

$$\Phi_i^N(s, t) = \phi_i^N(s, t) + \Delta\phi_i^N(s, t), \quad (\text{C1})$$

where $\Delta\phi_i^N$ corresponds to the boxlike diagrams. Analogously, for the fixed impact parameter amplitudes, we will have

$$\hat{\Phi}_i^N(s, b) = \hat{\phi}_i^N(s, b) + \Delta\hat{\phi}_i^N(s, b), \quad (\text{C2})$$

where, as explained in Sec. II C,

$$\begin{aligned} \Delta\phi_{\lambda''\mu''; \lambda\mu}^N(s, b) &= \frac{i}{2} \sum_{\lambda'''\mu'''} [\hat{\phi}_{\lambda''\mu''; \lambda'''\mu'''}^{\text{em}} \hat{\phi}_{\lambda'''\mu'''; \lambda\mu}^N(s, b) \\ &\quad + \hat{\phi}_{\lambda''\mu''; \lambda'''\mu'''}^N(s, b) \hat{\phi}_{\lambda'''\mu'''; \lambda\mu}^{\text{em}}(s, b)]. \end{aligned} \quad (\text{C3})$$

Evaluating (C3) in detail, we find for the $\hat{\Delta}\hat{\phi}_i^N(s, b)$

$$\begin{aligned} \Delta\hat{\phi}_1^N &= i(\hat{\phi}_1^{\text{em}} \hat{\phi}_1^N + \hat{\phi}_2^{\text{em}} \hat{\phi}_2^N + \hat{\phi}_5^{\text{em}} \hat{\phi}_5^N + \hat{\phi}_6^{\text{em}} \hat{\phi}_6^N), \\ \Delta\hat{\phi}_2^N &= i(\hat{\phi}_1^{\text{em}} \hat{\phi}_2^N + \hat{\phi}_2^{\text{em}} \hat{\phi}_1^N + \hat{\phi}_5^{\text{em}} \hat{\phi}_6^N + \hat{\phi}_6^{\text{em}} \hat{\phi}_5^N), \\ \Delta\hat{\phi}_3^N &= i(\hat{\phi}_3^{\text{em}} \hat{\phi}_3^N + \hat{\phi}_4^{\text{em}} \hat{\phi}_4^N + \hat{\phi}_5^{\text{em}} \hat{\phi}_5^N + \hat{\phi}_6^{\text{em}} \hat{\phi}_6^N), \\ \Delta\hat{\phi}_4^N &= i(\hat{\phi}_3^{\text{em}} \hat{\phi}_4^N + \hat{\phi}_4^{\text{em}} \hat{\phi}_3^N + \hat{\phi}_5^{\text{em}} \hat{\phi}_6^N + \hat{\phi}_6^{\text{em}} \hat{\phi}_5^N), \\ \Delta\hat{\phi}_5^N &= \frac{i}{2} [(\hat{\phi}_1^{\text{em}} + \hat{\phi}_3^{\text{em}}) \hat{\phi}_5^N + \hat{\phi}_5^{\text{em}}(\hat{\phi}_1^N + \hat{\phi}_3^N) \\ &\quad + (\hat{\phi}_2^{\text{em}} + \hat{\phi}_4^{\text{em}}) \hat{\phi}_6^N + \hat{\phi}_6^{\text{em}}(\hat{\phi}_2^N + \hat{\phi}_4^N)], \\ \Delta\hat{\phi}_6^N &= \frac{i}{2} [(\hat{\phi}_1^{\text{em}} + \hat{\phi}_3^{\text{em}}) \hat{\phi}_6^N + \hat{\phi}_6^{\text{em}}(\hat{\phi}_1^N + \hat{\phi}_3^N) \\ &\quad + (\hat{\phi}_2^{\text{em}} + \hat{\phi}_4^{\text{em}}) \hat{\phi}_5^N + \hat{\phi}_5^{\text{em}}(\hat{\phi}_2^N + \hat{\phi}_4^N)]. \end{aligned} \quad (\text{C4})$$

The b space transforms $\hat{\phi}_i^{\text{em}}(s, b)$, and $\hat{\phi}_i^N(s, b)$ are substituted into (C3) from Eqs. (B10), (B12), and (B13), and the actual correction amplitude $\Delta\phi_i^N(s, t)$ is then found using the transformation Eqs. (B2) and (B3).

The calculation is a massive one, so we shall only outline the main results. (Details are available upon request to the authors.)

The ‘‘contaminated’’ nuclear amplitudes Φ_i^N are defined by Eq. (C1). Remembering the definitions of $C_i(s, t)$, $A_i(s, t)$, etc. given in Eqs. (19), (20), (26), and (27), we express the corrections coming from $\Delta\phi_i^N(s, t)$ by setting

$$\begin{aligned} C_i(s, t) &= c_i(s, t) - \alpha \delta_i(s, t), \\ A_i(s, t) &= a_i(s, t) + \alpha \epsilon_i(s, t). \end{aligned} \quad (\text{C5})$$

It emerges that the infrared-singular term $\ln \lambda^2$ always occurs in the same form, namely,

$$\begin{aligned} \delta_i(s, t) &= a_i(s, t) F_1^A F_1^B \ln \lambda^2, \\ \epsilon_i(s, t) &= c_i(s, t) F_1^A F_1^B \ln \lambda^2. \end{aligned} \quad (\text{C6})$$

Thus, for this term, for every i ,

$$\Phi_i^N(s, t) = \phi_i^N(s, t) (1 + i \alpha F_1^A F_1^B \ln \lambda^2). \quad (\text{C7})$$

To the *given order in α* we may extract the factor $(1 + i \alpha F_1^A F_1^B \ln \lambda^2)$ from the *complete* expressions for the $\Phi_i^N(s, t)$ and we then assume that it represents the $O(\alpha)$ approximation to the phase factor $\exp(i \alpha F_1^A F_1^B \ln \lambda^2)$. We have not proved that the exponentiation really takes place but shall assume it on the basis of Ref. 9.

The $\ln \lambda^2$ term cancels out from all observables. We have derived expressions for $\delta_i(s, t)$, $\epsilon_i(s, t)$ valid for all t . Since, however, the parametrization of the nuclear amplitudes cannot be expected to hold at large t , our results cannot be trusted for large t . However, we are primarily interested in the region of small t , where the results are reliable, and detailed expressions for the $\delta_i(s, t)$ and $\epsilon_i(s, t)$, valid for small t , can be obtained from the authors.

The dominant, "enhanced $O(\alpha)$ " terms are given in Sec. IV.

APPENDIX D: CALCULATION OF THE CORRECTED ELECTROMAGNETIC AMPLITUDES

The corrected electromagnetic amplitudes are defined diagrammatically in Fig. 2. We shall only evaluate them for proton-proton scattering.

We write for these

$$\Phi_i^{\text{em}}(s, t) = \phi_i^{\text{em}}(s, t) + \Delta_i^{\text{em}}(s, t), \quad (\text{D1})$$

$$\hat{\Delta}\phi_1^{\text{em}} = \frac{i}{2} [(\hat{\phi}_1^{\text{em}})^2 + (\hat{\phi}_2^{\text{em}})^2 + 2(\hat{\phi}_5^{\text{em}})^2], \quad \hat{\Delta}\phi_2^{\text{em}} = i [\hat{\phi}_1^{\text{em}} \hat{\phi}_2^{\text{em}} + (\hat{\phi}_5^{\text{em}})^2],$$

$$\hat{\Delta}\phi_3^{\text{em}} = \frac{i}{2} [(\hat{\phi}_3^{\text{em}})^2 + (\hat{\phi}_4^{\text{em}})^2 + 2(\hat{\phi}_5^{\text{em}})^2], \quad \hat{\Delta}\phi_4^{\text{em}} = i [\hat{\phi}_3^{\text{em}} \hat{\phi}_4^{\text{em}} + (\hat{\phi}_5^{\text{em}})^2], \quad (\text{D4})$$

$$\hat{\Delta}\phi_5^{\text{em}} = i [(\hat{\phi}_1^{\text{em}} + \hat{\phi}_2^{\text{em}} + \hat{\phi}_3^{\text{em}} + \hat{\phi}_4^{\text{em}}) \hat{\phi}_5^{\text{em}}].$$

Our approach is similar to that used in Appendix C, though the calculation is much more subtle. Again, the results are very cumbersome, and details may be obtained from the authors.

Examination of the final results shows that each Φ_i^{em} is of the form

$$\Phi_i^{\text{em}}(s, t) = \phi_i^{\text{em}}(s, t) \left(1 + i\alpha \ln \frac{\lambda^2}{q^2} \right) + O(\alpha^2), \quad (\text{D5})$$

which to the given order in α can be written as

$$\Phi_i^{\text{em}}(s, t) = \phi_i^{\text{em}}(s, t) \exp\left(i\alpha \ln \frac{\lambda^2}{q^2}\right) [1 + O(\alpha)] \quad (\text{D6})$$

and, analogously, at fixed impact parameter,

$$\hat{\Phi}_i^{\text{em}}(s, b) = \hat{\phi}_i^{\text{em}}(s, b) + \hat{\Delta}\hat{\phi}_i^{\text{em}}(s, b), \quad (\text{D2})$$

where

$$\hat{\Delta}\hat{\phi}_{\lambda'\mu';\lambda\mu}^{\text{em}}(s, b) = \frac{i}{2} \sum_{\lambda''\mu''} \hat{\phi}_{\lambda'\mu';\lambda''\mu''}^{\text{em}}(s, b) \times \hat{\phi}_{\lambda''\mu'';\lambda\mu}^{\text{em}}(s, b). \quad (\text{D3})$$

Note that, in contrast to (C3), there is only one diagram contributing to $\Delta\phi^{\text{em}}$. In detail one has

We thus see that, independently of i , each helicity amplitude picks up the same phase factor. The infinite phase is dealt with as discussed in Appendix C and the phase $\exp(-i\alpha \ln q^2)$ is kept as the major correction factor, the *enhanced order* α correction, to the $\Phi_i^{\text{em}}(s, t)$.

In contrast to the corrections $\Delta\phi_i^N$, where the large inequalities of magnitude between different nuclear helicity amplitudes could lead to relatively enhanced $O(\alpha)$ corrections, here the $O(\alpha)$ terms in (D6) are never enhanced and can be neglected.

¹S. J. Lindenbaum, in *Proceedings of the Fourth Coral Gables Conference on Symmetry Principles at High Energy, University of Miami, 1967*, edited by A. Perlmutter and B. Kurşunoğlu (Freeman, San Francisco, 1967).

²J. Schwinger, *Phys. Rev.* **73**, 407 (1948).

³A. P. Vanzha, L. I. Lapidus, and A. V. Tarasov, *Yad. Fiz.* **16**, 1023 (1972) [*Sov. J. Nucl. Phys.* **16**, 565 (1973)]; B. Z. Kopeliovich and L. I. Lapidus, *Yad. Fiz.* **19**, 340 (1974) [*Sov. J. Nucl. Phys.* **19**, 168 (1974)].

⁴H. A. Bethe, *Ann. Phys. (N.Y.)* **3**, 190 (1958).

⁵L. D. Solov'ev, *Zh. Eksp. Teor. Fiz.* **49**, 292 (1965) [*Sov. Phys. -JETP* **22**, 205 (1966)].

⁶M. P. Locher, *Nucl. Phys.* **B2**, 525 (1967).

⁷G. B. West and D. Yennie, *Phys. Rev.* **172**, 1413 (1968).

⁸This distinction is strictly analogous to the difference between the Amati-Fubini-Stanghellini rules and the Abramovskii-Gribov-Kancheli cutting rules in Regge field theory.

⁹D. R. Yennie, S. C. Frautschi, and H. Suura, *Ann. Phys. (N.Y.)* **13**, 379 (1961).

¹⁰M. Jacob and G. C. Wick, *Ann. Phys. (N.Y.)* **7**, 404

(1959).

¹¹M. L. Goldberger, M. T. Grisaru, S. W. MacDowell, and D. Y. Wong, *Phys. Rev.* **120**, 2250 (1960).

¹²R. V. Kline, in *High Energy Physics with Polarized Beams and Targets*, proceedings of the Argonne Symposium, 1976, edited by M. L. Marshak (AIP, New York, 1977), p. 152.

¹³W. de Boer, R. C. Fernow, A. D. Krisch, H. E. Miettinen, T. A. Mulera, J. L. Roberts, K. M. Terwilliger, L. G. Ratner, and J. R. O'Fallon, *Phys. Rev. Lett.* **34**, 558 (1975). For a general outline of the new experiments, see A. D. Krisch, University of Michigan Report No. UM HE 76-38 (unpublished).

¹⁴This has been stressed by C. Bourrely and J. Soffer, *Lett. Nuovo Cimento* **19**, 569 (1977).

¹⁵W. Grein, R. Guigas, and P. Kroll, *Nucl. Phys.* **B89**, 93 (1975).

¹⁶The meaning of this so-called "experimental notation" for the observables is made clear in Sec. III D.

¹⁷I. P. Auer, E. Colton, D. Hill, K. Nield, B. Sandler, H. Spinka, Y. Watanabe, and A. Yokosawa, *Phys. Lett.* **67B**, 113 (1977).

$$\begin{aligned}
 \overline{\text{F}} &= \overline{\text{F}^{\text{em}}} + \overline{\text{f}^{\text{N}}} \\
 &+ \overline{\text{F}^{\text{em}} \text{f}^{\text{N}}} \\
 &+ \overline{\text{f}^{\text{N}} \text{F}^{\text{em}}}
 \end{aligned}$$

The diagram shows the relationship between amplitudes in the eikonal approximation. It consists of three rows of terms. The first row shows a circle labeled 'F' between two horizontal lines, followed by an equals sign, then a circle labeled 'F^{em}' between two horizontal lines, a plus sign, and a circle labeled 'f^N' between two horizontal lines. The second row shows a plus sign followed by two circles: the first is labeled 'F^{em}' and the second is labeled 'f^N', both between two horizontal lines. The third row shows a plus sign followed by two circles: the first is labeled 'f^N' and the second is labeled 'F^{em}', both between two horizontal lines. In the second and third rows, the two circles are connected by a vertical double line (representing a mass shell) between their top and bottom horizontal lines.

FIG. 1. Relationship between the pure nuclear, electromagnetic, and complete amplitudes in the eikonal approximation. Primed lines are on the mass shell.

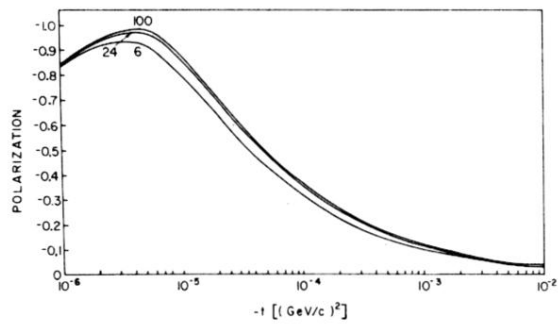


FIG. 10. Electromagnetically induced polarization P_n of the neutron in the reaction $np \rightarrow np$ at several laboratory momenta.

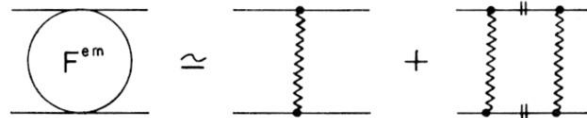


FIG. 2. Expansion of the complete electromagnetic amplitude F^{em} in powers of α .

The diagrammatic equation is as follows:

$$\begin{array}{c}
 \text{---} \\
 \bigcirc F^N \\
 \text{---} \\
 = \\
 \begin{array}{c}
 \text{---} \\
 \bigcirc f^N \\
 \text{---}
 \end{array}
 +
 \begin{array}{c}
 \text{---} \\
 \text{---} \\
 \text{---} \\
 \text{---} \\
 \text{---} \\
 \bigcirc f^N \\
 \text{---} \\
 \text{---} \\
 \text{---}
 \end{array} \\
 + \\
 \begin{array}{c}
 \text{---} \\
 \text{---} \\
 \text{---} \\
 \text{---} \\
 \text{---} \\
 \bigcirc f^N \\
 \text{---} \\
 \text{---} \\
 \text{---}
 \end{array}
 \end{array}$$

Detailed description: The equation defines the "contaminated" nuclear amplitude F^N . On the left is a circle labeled F^N with two horizontal lines passing through its center. This is equal to the sum of three terms. The first term is a circle labeled f^N with two horizontal lines passing through its center. The second term is a circle labeled f^N with two horizontal lines passing through its center, and a vertical wavy line connecting the top and bottom lines to the right of the circle. The third term is a circle labeled f^N with two horizontal lines passing through its center, and a vertical wavy line connecting the top and bottom lines to the left of the circle.

FIG. 3. Definition of the "contaminated" nuclear amplitude F^N .

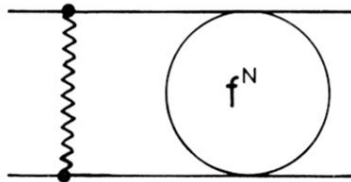


FIG. 4. Feynman-diagram analog of a correction term in F^N .

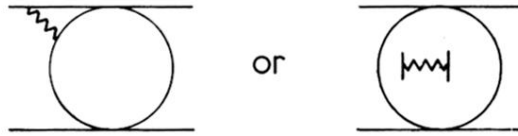


FIG. 5. Examples of electromagnetic corrections not taken into account.

$$\Phi^N = \begin{array}{c} \lambda \quad \lambda' \\ \text{---} \quad \text{---} \\ \text{---} \quad \text{---} \\ \mu \quad \mu' \end{array} \begin{array}{c} \circ \\ \phi^N \\ \circ \end{array} + \sum_{\lambda'' \mu''} \begin{array}{c} \lambda \quad \lambda'' \quad \lambda' \\ \text{---} \quad \text{---} \quad \text{---} \\ \text{---} \quad \text{---} \quad \text{---} \\ \mu \quad \mu'' \quad \mu' \end{array} \begin{array}{c} \circ \\ \phi^N \\ \circ \end{array} + \begin{array}{c} \lambda \quad \lambda'' \quad \lambda' \\ \text{---} \quad \text{---} \quad \text{---} \\ \text{---} \quad \text{---} \quad \text{---} \\ \mu \quad \mu'' \quad \mu' \end{array} \begin{array}{c} \circ \\ \phi^N \\ \circ \end{array}$$

FIG. 6. Definition of the "contaminated" nuclear amplitudes for spin- $\frac{1}{2}$ particles.

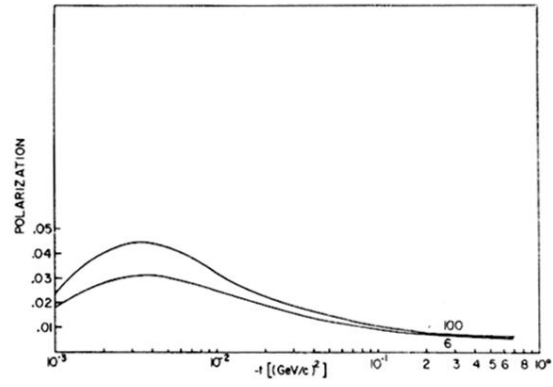


FIG. 7. Electromagnetically induced polarization in proton-proton scattering at laboratory momenta of 6 and 100 GeV/c.

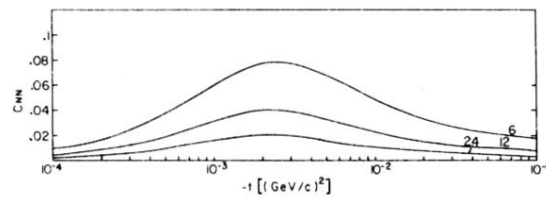


FIG. 8. Electromagnetically induced spin correlation parameter C_{NN} at $p_{\text{lab}} = 6, 12,$ and $24 \text{ GeV}/c$.

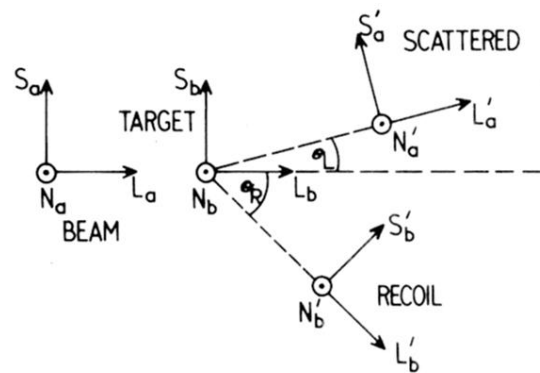


FIG. 9. Definition of the polarization directions N , L , S for the various particles in the reaction $A + B \rightarrow A' + B'$, all in the laboratory frame.